**Title**

# Welcome pathogens: transient heat dampens the responses to acibenzolar-*S*-methyl beyond defenses in apple plants

**Authors**

Erwan Chavonet[1,†,‡], Bao-huynh Nguyen[1,‡], Christelle Heintz[1], Raphaël Cournol[1], Jitka Široká[2], Ondřej Novák[2], Romain Larbat[1], Matthieu Gaucher[1], Marie-Noëlle Brisset[1], Florent Pantin[1,*], Alexandre Degrave[1,*]

[1]Institut Agro, Univ Angers, INRAE, IRHS, SFR QuaSav, 49000, Angers, France
[2]Laboratory of Growth Regulators, Institute of Experimental Botany of the Czech Academy of Sciences & Palacký University, Šlechtitelů 27, 78371 Olomouc, Czech Republic
[†]Present address: Laboratoire de Biogenèse Membranaire, CNRS, Université de Bordeaux, Villenave d'Ornon, France.
[‡]Co-first authors.
*Authors for correspondence:
Florent Pantin florent.pantin@institut-agro.fr
Alexandre Degrave alexandre.degrave@institut-agro.fr

Word counts for the main sections: 7 183
Number of figures: 11 (all in colour)
Number of tables: 0
Supporting information: 5 supplementary figures and 2 supplementary tables

## Summary

- Climate change affects plant-pathogen interactions, with disease outcome varying depending on pathosystem and environmental scenario. In Arabidopsis, a thermo-sensitive module of salicylic acid (SA) signaling makes immunity vulnerable to heat. The potent resistance inducer acibenzolar-*S*-methyl (ASM), an SA analogue that up-regulates transcription of defense genes, could restore plant protection under heat but not core SA signaling. Here, we investigated how high temperature rewires the ASM-induced responses of the apple immune system.
- We treated apple plants with ASM under contrasting heatwave scenarios and subsequently exposed them to *Erwinia amylovora* (the fire blight bacterium) or *Venturia inaequalis* (the apple scab fungus) while monitoring gene expression.
- While pre-exposing apple plants to high temperature did not change their susceptibility to pathogens, it drove a loss of ASM-induced protection. Transcriptomic analysis revealed broad dampening of ASM-regulation upon high temperature, for a wide range of biological processes beyond defense. We uncovered thermo-sensitive “resistance” and “susceptibility” marker genes with ASM-responsiveness being critically vulnerable to heat.
- We concluded that exposure to heatwave prevents ASM from fully mounting its protective responses in apple, not only lowering defenses but also offering more favorable hosting conditions. Our work highlights plant immunity as the joint outcome of resistant and susceptible responses.



## Key words

Acibenzolar-*S*-methyl (ASM), defenses, *Erwinia amylovora* (fire blight), heat, immunity, *Malus domestica* (apple), susceptibility, *Venturia inaequalis* (apple scab)

**ORCIDs**

| | |
|---|---|
| Erwan Chavonet | 0009-0006-4985-5255 |
| Bao-huynh Nguyen | 0009-0004-4221-2885 |
| Jitka Široká | 0000-0002-4988-2919 |
| Ondřej Novák | 0000-0003-3452-0154 |
| Romain Larbat | 0000-0002-9060-5040 |
| Matthieu Gaucher | 0000-0003-2730-0639 |
| Marie-Noëlle Brisset | 0000-0002-5139-3292 |
| Florent Pantin | 0000-0003-0636-1061 |
| Alexandre Degrave | 0000-0002-5642-3235 |


**Plain language summary**

Resistance inducers may be applied on crops to boost their immunity against pathogens – just like vaccines for humans. Working on apple plants treated with a resistance inducer, we found that heatwaves “disarm” plant’s ability to mount an effective immune response against two major diseases, fire blight and apple scab. Heatwaves not only prevent full expression of plant defenses, but also favor a physiological status that is beneficial to the pathogens.

## Introduction

Climate change modifies the many interactions between plants and pathogens. The 'disease triangle' framework posits that successful disease establishment requires a virulent pathogen, a susceptible host plant and favorable environmental conditions (Stevens, 1960; Velásquez *et al.*, 2018; Roussin-Léveillée *et al.*, 2024). Changes in temperature, radiation, relative humidity, soil water content and atmospheric $CO_2$ concentration may all affect the physiology and development of plants and pathogens, either directly or through their mutual interaction. For instance, temperature elevation has profound effects on plants, triggering thermomorphogenesis (Quint *et al.*, 2016), acceleration of phenology and growth (Parent *et al.*, 2010), alteration of carbon balance (Vasseur *et al.*, 2011), tissue desiccation (Marchin *et al.*, 2022) or even burning (Coupel-Ledru *et al.*, 2024), depending on the range and duration of temperature increase, the genetic background and the influence of other environmental factors (Long & Ort, 2010). Temperature elevation may also affect different components of the plant immune system, either positively or negatively (Malamy *et al.*, 1992; Zhu *et al.*, 2010; Cheng *et al.*, 2013; Zhang *et al.*, 2017; Richard *et al.*, 2020; Qiu *et al.*, 2022; Kim *et al.*, 2022). In turn, temperature elevation largely affects the growth rate and virulence of microbes, resulting in positive or negative effects depending on the species and strain, with feedback from host responses (Velásquez *et al.*, 2018; Roussin-Léveillée *et al.*, 2024). Thus, warming may confer more or less chance to a given microbe to meet and infect a susceptible plant, depending on the pathosystem and the environmental scenario (Desaint *et al.*, 2021; Chaloner *et al.*, 2021).

Focusing on the model pathosystem *Arabidopsis thaliana* / *Pseudomonas syringae*, recent reports have established that plant immunity is vulnerable to heat (28–30°C), through a negative effect on salicylic acid (SA) – the major hormone of plant defense (Peng *et al.*, 2021). Such vulnerability arises from a thermosensitive pair of master transcription factors (CBP60g and its paralogue SARD1) that fails to induce the expression of SA biosynthesis genes upon heat, making host plants more susceptible (Huot *et al.*, 2017; Kim *et al.*, 2022; Shields *et al.*, 2023). From the pathogen's perspective,

112 elevated temperature also enhances virulence by accelerating translocation of bacterial
113 effector proteins, leading to more severe disease under heat (Huot *et al.*, 2017). However,
114 over- or targeted- expression of *CBP60g* is sufficient to restore thermo-resilient SA
115 production and effective defense (Kim *et al.*, 2022), which suggests that loss of host SA
116 synthesis is the major driver of enhanced disease under heat within this pathosystem.
117 Application of acibenzolar-*S*-methyl (ASM, also known as BTH) effectively prevents
118 bacterial infection at warm temperature but, interestingly, does not restore the SA pathway
119 (Huot *et al.*, 2017). ASM is a long-standing plant resistance inducer that is converted *in*
120 *planta* into acibenzolar, a biologically active form that shares functional and structural
121 analogies with SA (Görlach *et al.*, 1996; Canet *et al.*, 2010a; Tripathi *et al.*, 2010). While
122 free or bound SA may accumulate upon ASM application in some species and
123 environmental conditions (e.g. Kuźniak *et al.*, 2014; Huot *et al.*, 2017; Ullah *et al.*, 2019;
124 Ratchaseema *et al.*, 2021), there is clear evidence that SA accumulation is dispensable
125 for efficient ASM-induced protection (Friedrich *et al.*, 1996; Lawton *et al.*, 1996; Canet *et*
126 *al.*, 2010a; Huot *et al.*, 2017). By contrast, ASM-induced protection critically requires
127 NPR1 (NONEXPRESSER OF PR GENES 1; Lawton *et al.*, 1996; Canet *et al.*, 2010a,b;
128 Huot *et al.*, 2017), now known as the SA receptor acting as a transcriptional co-activator
129 (Ding *et al.*, 2018). It is therefore likely that NPR1 directly recognizes acibenzolar to
130 activate downstream defense genes such as the canonical SA marker *PR1*
131 (*PATHOGENESIS-RELATED GENE 1*). In Arabidopsis at elevated temperature, applying
132 ASM properly initiates NPR1 signaling and yet fails to induce *PR1* expression and
133 feedforward SA accumulation (Huot *et al.*, 2017). This suggests that ASM can
134 counterbalance heat-sensitive immunity via other routes than the core SA pathway.
135
136 It is noteworthy, yet, that ASM regulates the transcription of hundreds of genes with
137 biological roles beyond defense, for instance by down-regulating genes related to
138 metabolism, photosynthesis or cell division (Huot *et al.*, 2017; Warneys *et al.*, 2018).
139 Among these processes that are routinely sustained by plants for their physiology and
140 development, some may involve susceptibility factors that are exploited by pathogens to
141 facilitate colonization and propagation *in planta* (Eckardt, 2002; van Schie & Takken,
142 2014; Gorshkov & Tsers, 2022). Thus, it is perhaps useful to consider plant immunity as

143 the joint outcome of resistant (R) and susceptible (S) responses. In this framework, ASM-
144 induced immunity would result from both the enhancement of defense genes and the
145 repression of susceptibility genes, with different effects on immunity, physiology and
146 development, depending on the species and the environment. To what extent high
147 temperature may affect the different components of ASM-induced immunity remains
148 largely unexplored.
149
150 We addressed this question on apple (*Malus domestica*), where ASM effectively controls
151 immunity by eliciting the production of defense compounds such as pathogenesis-related
152 (PR) proteins, and promotes resistance against several pests (Brisset *et al.*, 2000;
153 Maxson-Stein *et al.*, 2002; Dugé de Bernonville *et al.*, 2014; Aćimović *et al.*, 2015;
154 Marolleau *et al.*, 2017; Warneys *et al.*, 2018; Chavonet *et al.*, 2022). These include *Erwinia*
155 *amylovora*, a bacteria responsible for fire blight (Vanneste, 2000), and *Venturia*
156 *inaequalis*, a fungus responsible for apple scab (Bowen *et al.*, 2011). Both pathogens
157 exclusively infect young organs, yet their infection routes and pathogenic mechanisms
158 differ. Following penetration through natural pores or wounds of young leaves or flowers,
159 *E. amylovora* colonizes host apoplast by feeding on intracellular content spilling out from
160 cell death induced by bacterial type III effectors (Zeng *et al.*, 2021) and causes progressive
161 necrosis along the stem – potentially leading to tree death. Exudation of ooze droplets
162 from infected tissues is responsible for secondary infections. By contrast, germ tubes from
163 ascospores of *V. inaequalis* penetrate the cuticle of developing leaves or fruits, either
164 directly or through an appressorium, before forming stromata that extract plant nutrients
165 from the subcuticular space. Stromata then produce conidia that are spread by wind and
166 rain, originating secondary infections that occur throughout fruit development, leading to
167 necrotic lesions that render the fruits unmarketable (Bowen *et al.*, 2011). Most commercial
168 apple cultivars are susceptible to *E. amylovora* (Kostick *et al.*, 2019) and *V. inaequalis*
169 (Gessler *et al.*, 2006; Holb, 2007). The application of resistance inducers such as ASM is
170 a promising strategy to manage the protection of susceptible orchards against these two
171 diseases at least. Nonetheless, the efficacy of resistance inducers depends on
172 environmental conditions (Walters *et al.*, 2005, 2013; Sandroni *et al.*, 2020) – and the
173 components of immunity that are susceptible to the environment remain to be identified.

174

175 Here, we found that the efficacy of ASM protection against *E. amylovora* and *V. inaequalis*
176 erodes when apple plants are pre-exposed to transient heat. Such vulnerability to heat
177 was not accompanied by misregulation of master defense modules, contrasting with
178 Arabidopsis. Instead, transcriptomic analyses revealed that transient heat triggered
179 pervasive dampening of ASM-induced transcriptional regulation on a wide range of
180 physiological processes, leaving apple plants less immune. Thus, transient heat 'imprints'
181 the physiology of apple plants so that ASM-induced immunity becomes less protective
182 against pathogens in these conditions.

183

184 **Materials and Methods**

185

186 *Plant materials and growth conditions*

187 Experiments were performed on apple seedlings (3–6 leaves) obtained from seeds of
188 open-pollinated trees of cv. Golden Delicious, or on scions (2 to 6-month-old) of Golden
189 Delicious doubled-haploid 13 (GDDH13; Daccord *et al.*, 2017) grafted on the MM106
190 rootstock. Plants were cultivated in semi-controlled greenhouse conditions (natural
191 photoperiod supplemented with artificial light to reach a 16-h photophase, 23–25°C day,
192 17°C night, watering every 2–4 days) in individual pots filled with a growing medium
193 (Neuhaus Huminsubstrat N4, Klasmann-Deilman France, Bourgoin-Jallieu, France). Both
194 seedlings and grafted plants were chosen for protection experiments because of their
195 overall susceptibility to fire blight and apple scab, and transcriptomic analyses were
196 conducted on GDDH13 grafted scions to take advantage of the high-quality genome
197 sequence of this homozygous genotype (Daccord *et al.*, 2017). In all experiments, the
198 youngest unfolded leaf at time of treatment application was identified by attaching a small
199 clip to the petiole just before spraying ASM or water.

200

201 *Temperature and chemical treatments*

202 Temperature scenarios were applied in environmental chambers FitoClima 600 (ARALAB,
203 Rio de Mouro, Portugal) with controlled temperature, relative humidity (RH) and radiation
204 provided by white, blue and red LED tubes. In a first set of experiments, plants were

205 exposed to constant temperature (20°C) and RH (60%) day and night (12-h photoperiod
206 at 300 µmol $m^{-2}$ $s^{-1}$). Heat was imposed by switching temperature to 35°C during 24 h or
207 during the 12-h photophase, depending on the experiment as described in the Results
208 section. In the following experiments, the environmental scenarios were refined to match
209 natural fluctuations, based on the average temperature dynamics on the 11 hottest days
210 (peak at 34–36°C) between March and July 2016–2018 in an experimental orchard
211 (UE449 HORTI, INRAE, Beaucouzé, France) adjacent to our research center (Fig. S1). A
212 typical heat day was designed through piecewise linear approximation of temperature,
213 relative humidity and irradiance over time, with a 4-h heat plateau in the afternoon ("Short"
214 settings") to be compared to standard conditions for apple tree growth in the same French
215 area ("Control" settings") and to an artificially extended 12-h heatwave ("Long" settings)
216 (Fig. S2). Nighttime temperature was set at 18°C until 8:00 am, followed by a 2-h ramp
217 and a 12-h plateau at 21°C and 35°C for the "Control" and "Long" settings, respectively,
218 or a 6-h ramp and a 4-h plateau at 35°C for the "Short" setting. Finally, a 2-h ("Control"
219 and "Long") or a 6-h ("Short") decreasing ramp was applied to reach 18°C at midnight. To
220 match natural variations, RH was covaried with temperature, reaching 80%, 60% and 40%
221 when temperature was 18°C, 21°C and 35°C, respectively (Fig. S2). The same daily
222 fluctuations in radiation were applied to the three regimes, based on the radiation
223 measured in the orchard. Lighting progressively started at 8:00 am to reach
224 300 µmol $m^{-2}$ $s^{-1}$ between midday and 4:00 pm, and progressively declined to switch off
225 at 8:00 pm. The number of days of heat vs. control temperatures depended on the
226 objective of experiment, and each scenario is described in Results for each experiment.

227 Acibenzolar-*S*-methyl (ASM) solutions were prepared from the commercial product Bion®
228 50WG (Syngenta, Basel, Switzerland; 50% of ASM) in reverse osmosis water at 0.4 g $L^{-1}$.
229 The same water was systematically used as control. Aerial parts of plants were sprayed
230 until incipient runoff with a spray gun Aeryo-1.4 (Deltalyo, Mably, France) between
231 8:00 am and 10:00 am on the day selected for the treatment. The timing of treatment in
232 relation to temperature scenario depended on the experiment and is described in Results.

233

234 *Quantification of ASM in treated leaves*

235 The morning of the experiment, seedlings from the greenhouse were sprayed with ASM
236 ($t_0$) and immediately transferred in ARALAB chambers at 20°C or 35°C (60% RH,
237 300 µmol $m^{-2}$ $s^{-1}$ PAR). After 6 h, when all leaves were unequivocally dry, the youngest
238 unfolded leaf was harvested on 2 plants, rinsed 3 times in water, dried with paper towel,
239 pooled in an Eppendorf and frozen in liquid nitrogen. This protocol was repeated on the
240 leaf insertion rank immediately below. For each leaf rank and each temperature, 10
241 replicates were obtained. Pooled samples were crushed to a fine powder with mortar and
242 pestle. Fresh leaves powders (50 mg) were suspended in 500 µL of methanol spiked with
243 0.2 µg $mL^{-1}$ of [$^2H_6$]ABA as internal standard. After 10 s vortexing, mixtures were stored
244 for 15 h at –20°C and then centrifuged at 10000 g for 10 min at 4°C. The supernatant was
245 collected and the pellet extracted a second time with 500 µL of methanol. The two
246 combined supernatants were then evaporated using a vacuum concentrator. Dried
247 extracts were resuspended in 200 µl of methanol, filtered (0.2 µm) and transferred to vials
248 before LC-MS analysis.
249 Chromatographic analyses were performed on a Vanquish Flex UHPLC system equipped
250 with a quaternary solvent manager, an autosampler and a temperature-controlled column.
251 ASM and metabolites contained in the extracts (1 µL) were separated on a HSS-T3
252 column (100 × 2.1 mm, 1.8 µm) (Waters, Milford, MA, USA) using a gradient of mobile
253 phase composed of water + 0.1% formic acid (A) and methanol + 0.1% formic acid (B) at
254 a flow rate of 300 µL $min^{-1}$. The samples were kept at 10°C and the column was
255 maintained at 25°C. The elution program consisted in a first 2-min step with 0% B, then a
256 linear ramp from 0% to 100% B in 18 min, followed by a 3-min step with 100% B, before
257 re-equilibrating the column in the initial conditions for 7 min. The samples were analyzed
258 randomly.
259 $MS^1$ detection was performed on a TSQ Quantis Plus™ (ThermoFisher Scientific,
260 Bremen, Germany) mass spectrometer in positive and negative electrospray ionization
261 (ESI) modes. The capillary voltages were set at 3 kV and 2.75 kV for positive and negative
262 modes, respectively. The source gases were set (in arbitrary unit $min^{-1}$) to 40 (sheath
263 gas), 10 (auxiliary gas) and 0 (sweep gas) and the vaporizer temperature was 280°C. Full
264 scan $MS^1$ spectra were acquired from 50 to 700 *m/z* with a scan rate of 1000 Da $s^{-1}$. ASM
265 was quantified in selective ion monitoring (SIM) mode by following ion at *m/z* 211 in

266 positive mode. Acibenzolar acid was monitored at *m/z* 179 in negative mode together with
267 the internal standard [$^2H_6$]ABA at *m/z* 269. ASM, acibenzolar acid and [$^2H_6$]ABA pure
268 standards eluted at 18.1 min, 14.1 min and 19.7 min, respectively, with the above-
269 mentioned conditions. ASM and acibenzolar acid quantities in dry laminas were
270 determined using respective standard curves. Control leaves were also harvested at $t_0$
271 (without any spray) from independent plants in the greenhouse, and all samples were
272 below the detection limit.
273
274 *Physiological measurements*
275 The morning of the experiment, each plant was first characterized in the greenhouse.
276 Stem height (from the cotyledon to the apical meristem) and lamina length (youngest
277 unfolded leaf, just identified using a clip) were measured using a ruler. Stomatal
278 conductance ($g_s$) of the clipped leaf and of the leaf immediately below (more mature and
279 less susceptible to *E. amylovora* and *V. inaequalis*) was determined using a porometer
280 (LI-600; Li-COR Inc., Lincoln, NE, USA). Plants were then treated with ASM or water ($t_0$)
281 and immediately placed in ARALAB chambers at 12-h photoperiod, 250–300 µmol $m^{-2}$ $s^{-1}$
282 PAR, and 60% RH. Air temperature was maintained at either 20°C or 35°C for 24 h. $g_s$ of
283 both leaves were measured again at 24, 48 and 72 h after treatment. Stem height and
284 lamina length of the clipped leaf were measured again at 72 h after treatment and absolute
285 elongation rates were computed as the difference between initial and final lengths divided
286 by the time interval.
287
288 *Pathogen strains and protection experiments*
289 Plants were inoculated by the CFBP1430 strain of *E. amylovora* (Paulin & Sampson,
290 1973). Inoculum was suspended at $10^8$ cfu $mL^{-1}$ in reverse osmosis water from an
291 exponential growth phase culture cultivated overnight at 26°C on solid King's B medium
292 (King *et al.*, 1954). Inoculation was carried out in greenhouse conditions (1 or 3 d following
293 ASM treatment for seedlings, and 3 d after ASM treatment for grafted plants), by cutting
294 two-thirds of the two youngest unfolded leaves (perpendicularly to the midrib) with scissors
295 previously dipped in the inoculum. Progressions of necroses from the inoculated leaves
296 to the stems, through the midrib and petiole, were assessed 21 or 28 d post-inoculation

297 for seedlings or grafted plants, respectively. Disease incidence was calculated as the
298 percentage of diseased plants, considering that a plant was diseased when typical fire
299 blight necrosis reached the stem, whereas it was considered healthy if no necrosis
300 occurred or if necrosis was restricted to the inoculated leaf (including its petiole) at the
301 end of the experiment.

302 The *V. inaequalis* strain 104 (Guillaumès *et al.*, 1995) was prepared in reverse-osmosis
303 water from scabbed apple leaves previously stored at –80 °C. The suspension was
304 roughly filtered to remove debris, adjusted to a concentration of $1.5 \times 10^4$ conidia $mL^{-1}$ and
305 sprayed onto apple seedlings until incipient runoff. To facilitate conidial germination and
306 fungus penetration, plants were then placed in a controlled environmental room in the
307 dark, at 18°C and with humidity maintained above 90% for 48 h. Light was then switched
308 on (16-h photoperiod), and humidity reduced to 70% while temperature was maintained
309 at 18°C. Symptoms were assessed 21 d after inoculation on the youngest unfolded leaf
310 at the time of ASM application. Disease incidence was calculated as the percentage of
311 diseased plants, considering that a plant was diseased when visible sporulation occurred
312 on the target leaf.

313 The numbers of independent trials and biological replicates are indicated in the figure
314 legends.

315

316 *Sampling for gene expression and protein analyses*

317 Sampling for gene expression or protein analysis was carried out by pooling the youngest
318 unfolded leaf (or its distal two-thirds cut out while inoculating *E. amylovora*) from 1 to 5
319 plants to form one replicate. Samples were immediately frozen in liquid nitrogen and
320 stored at -80°C before processing. The genetic material (Golden Delicious seedling or
321 GDDH13 grafted plants) as well as the number of biological replicates and independent
322 experiments are indicated in the figure legends.

323

324 *Microarray procedure*

325 Leaves were ground in fine powder (Retsch, Haan, Germany) and total RNA was
326 extracted from about 200 mg using the Nucleospin RNA Plant Kit (Macherey-Nagel,
327 Düren, Germany) according to the manufacturer's protocol. Samples purity and
328 concentration were assayed with the Agilent 2100 bioanalyzer system and the RNA 6000
329 Nano LabChip kit (Agilent Technologies, Waldbroon, Germany) according to the
330 manufacturer's recommendation. Two hundred ng of RNA were amplified and labelled as
331 described in Perrin *et al.* (2020). Labelled cDNA were prepared for hybridization according
332 to the manufacturer's procedure with the Gene Expression Hybridization Kit (Agilent,
333 Waldbronn, Germany) and the Hi-RPM gene Expression Hybridization Kits (Agilent,
334 Waldbronn, Germany) and hybridized on AryANE v1.1 slides (Agilent, design n°85275) in
335 incubation chambers for 17 h at 65°C. After washing, slides were scanned at 3 µm with
336 an Innoscan 710 using Innoscan v3.4.7 software (Innopsys, Carbonne, France).

337

338 *Transcriptional marker analysis*

339 Leaves were ground and total RNA were extracted as described above in the microarray
340 procedure, except that RNA purity and concentration were assessed with a NanoDrop
341 One (Thermo Fisher Scientific, Waltham, MA, USA). Reverse transcription (RT) and
342 quantitative polymerase chain reaction (qPCR) were performed as described in Chavonet
343 *et al.* (2022). The primers and their targets designed for this study are listed in Table S2;
344 while the remaining ones are described in Dugé de Bernonville *et al.* (2014). The relative
345 changes in gene expression were calculated using the $2^{-\Delta\Delta CT}$ method (Schmittgen & Livak,
346 2008) with normalization against three internal reference genes (Vandesompele *et al.*,
347 2002). The mean expression value calculated from samples obtained on water-treated
348 plants exposed to control temperature (or 3-d heatwave for the experiments on heat wave
349 duration and positioning) was used as the calibrator to compute the relative expression
350 as $\log_2$ ratios.

351

352 *Protein extraction, separation and immunodetection*

353 Two hundred mg of deep-frozen leaf powder were used for phenolic extraction of protein
354 and their subsequent solubilization, as described in Chavonet *et al.* (2022). Ten µg of total

355 protein extracts were separated on 1D SDS-PAGE, electroblotted onto 0.45 mm
356 polyvinylidene difluoride (PVDF) membranes (immobilon-P, Milli- pore Corp., Bedford,
357 MA, United States) as described in Warneys *et al.* (2018). Immunodetection of target
358 proteins was performed using the rabbit primary antibodies described in Chavonet *et al.*
359 (2022) using the procedure from Warneys *et al.* (2018).

360

361 *Quantification of salicylates*

362 Salicylic acid (SA), SA glucoside (SAG) and SA glucose ester (SGE) in laminas of apple
363 seedlings were quantified in precisely weighed freeze-dried samples (1.8 ± 0.02 mg DW).
364 Samples were extracted in 1 mL of 1 mol $L^{-1}$ formic acid in 10% aqueous methanol with
365 a stable isotope-labeled internal standard ([$^2H_4$]SA at 20 pmol per sample), following
366 Široká *et al.* (2022). Extracts were purified with HLB Oasis® SPE columns (Waters) as
367 described by Floková *et al.* (2014). SA was analysed on an Agilent 1290 Infinity LC system
368 coupled to a 6490 Triple Quadrupole LC/MS, following Široká *et al.* (2022). SAG and SGE
369 were determined from the same samples on an ACQUITY UPLC H-Class PLUS system
370 linked to a Xevo TQ-S micro triple-quadrupole MS (Waters), operating in negative
371 ionization multiple reaction monitoring mode (quantification: 299 > 137, collision energy
372 12 eV, cone voltage 30 V; confirmation: 299 > 93, collision energy 34 eV, cone voltage
373 28 V). Separation was performed on an Acquity UPLC BEH Shield C18 column
374 (2.1 × 150 mm, 1.7 µm, Waters) at 40°C. The mobile phase consisted of 0.3% aqueous
375 formic acid (A) and methanol (B), with a flow rate of 0.3 mL $min^{-1}$ and a linear gradient
376 from 5% to 98% B within 10 min. The determination of SAG and SGE was semi-
377 quantitative, using [$^2H_4$]SA as internal standard.

378

379 *Data analysis*

380 Data analysis was performed using R (version 4.2.0; R Development Core Team, 2022)
381 and RStudio (version 2024.09.0; R Studio Team, 2024) software except for Clustering
382 Affinity Search Technique (CAST). Multiple comparisons on proportion of diseased and
383 healthy plants were performed using pairwise Fisher's exact tests of the "rstatix" package
384 (version 0.7.2; Kassambara, 2023a). Two-way ANOVA and estimation of the effect sizes

385 ($\eta^2_g$) of individual factors (treatment and temperature) and their interaction were performed
386 using the same package. Multiple comparisons on expression values were performed with
387 a Tukey's HSD test from package "stats" (R Development Core Team, 2022). Multiple
388 comparisons on growth and conductance data were performed with pairwise t-tests
389 adjusted by the Bonferroni method using "rstatix" (Kassambara, 2023a). Statistical
390 differences for multiple comparisons were established with a risk threshold of 5%
391 designated by different letters using package "rcompanion" (version 2.4.36; Mangiafico,
392 2024). For microarrays, data normalization and statistical analyses were performed using
393 the LIMMA 3.10.1 package (Smyth, 2005) from the Bioconductor project, following Celton
394 *et al.* (2014). Briefly, after extraction of the scan values with Mapix (version 8.2.5;
395 Innopsys, Carbonne, France), the data were normalized with the lowess method, and
396 differential expression analyses were performed using the lmFit function and Bayes
397 moderated t test. Genes were considered differentially expressed (DEGs) for |log2 ratios|
398 ≥ 1 and p-value ≤ 0.05. Pathway enrichment analysis was performed on all genes dataset
399 without applying filtering with the Gene Set Enrichment Analysis (GSEA, 10000
400 permutations) by ranked genes by their $\log_2$ fold-change ratio (Subramanian *et al.*, 2005)
401 with Benjamini and Hochberg procedure for controlling false discovery rate (Hung *et al.*,
402 2012), available with the package "ClusterProfiler" (version 4.4.4; Wu *et al.*, 2021). CAST
403 was performed on genes corresponding to DEGs in at least one of the comparisons by
404 the software MeV (Multi Experiment Viewer) with Pearson correlation distance metric and
405 an affinity threshold of 0.95 (Ben-Dor *et al.*, 1999; Saeed *et al.*, 2003). Graphical
406 representations were generated using the package "ggplot2" (version 3.5.1; Wickham,
407 2016) associated with "ggpubr" (version 0.6.0; Kassambara, 2023b). Heatmaps were
408 performed with "ComplexHeatmap" (version 2.18.0; Gu, 2022). Principal Component
409 Analysis (PCA) were carried out with packages "FactoMineR" (version 2.8; Lê *et al.*, 2008)
410 and "factoextra" (version 1.0.7; Kassambara & Mundt, 2020).
411
412
413 **Results**
414
415 *High temperature impedes the protecting effect of ASM against fire blight and apple scab*

416

417 To explore the interaction between high temperature and ASM-induced immunity by
418 excluding any direct effect of temperature on pathogen growth or virulence, we targeted
419 ASM and/or heat applications prior to pathogen inoculation. We first sprayed apple
420 seedlings with ASM (or water) and immediately exposed them to a sudden temperature
421 elevation at 35°C during 24 h (or to a 20°C constant regime) as depicted in Fig. 1a (left
422 part). Transient heat and ASM treatments had no obvious impact on plant phenotype, as
423 illustrated by growth or stomatal conductance that remained unaffected, either on the
424 youngest unfolded leaf at the time of ASM application or in the leaf immediately below
425 (Fig. S3). Three days after this dual prior treatment, we inoculated the newly unfolded leaf
426 with *E. amylovora* before assessing fire blight symptoms for three weeks. High
427 temperature *per se* did not enhance the susceptibility of apple plants to fire blight in water-
428 treated seedlings (Fig. 1b). However, high temperature abolished the protecting effect of
429 ASM that was observed at control temperature. Similar results were obtained when
430 seedlings were exposed to a close environmental scenario and further inoculated with *V.*
431 *inaequalis* (Fig. 1c).

432

433 To check if this loss of ASM efficiency at high temperature could be observed in more
434 realistic environmental conditions, we devised new scenarios based on records from a
435 local meteorological station that corresponded to heatwave periods (Methods). We varied
436 the duration of heat (numbers of days in the heatwave, and number of heat hours within
437 a day) and inoculated the youngest unfolded leaf with *E. amylovora* systematically 1 d
438 after ASM treatment (Fig. 2a). We found that applying a short heatwave with a 4-h plateau
439 at 35°C during the photophase for 3 d induced a large loss of ASM-efficiency, similar to
440 that in the previous experiment (Fig. 2b). Applying the same heatwave for only one day
441 before inoculation was not sufficient to impede the effect of ASM. Nonetheless, when the
442 heat plateau was extended to 12 h for a single day, ASM lost again most of its protecting
443 effect. Altogether, these results show that accumulation of high temperatures prior to
444 inoculation impairs the ability of apple plants to mount an effective ASM-induced
445 protection against *E. amylovora* and *V. inaequalis*.

446

447 *High temperature does not impair ASM uptake or SA metabolism*

448 One trivial explanation might be that high temperature prevents correct uptake of ASM,
449 due to e.g. enhanced evaporation and thus reduced leaf humectation. However, ASM
450 content in treated leaves of apple seedlings 6 h after spraying (after complete evaporation)
451 was similar at 20°C and 35°C (Fig. 3a). Moreover, acibenzolar acid, the first catabolite of
452 ASM that is biologically active (Tripathi *et al.*, 2010), was significantly enhanced at 35°C
453 (Fig. 3b). This shows that ASM uptake and metabolism are operational at high
454 temperature.

455

456 We also checked whether transient heat could alter SA metabolism, as observed in
457 Arabidopsis (Huot *et al.*, 2017; Kim *et al.*, 2022). In apple seedlings exposed to control
458 temperature, ASM did not induce SA accumulation 3 d after application, either in the
459 youngest unfolded leaf at time of ASM spraying (Fig. 3c, left), or in the leaf above that had
460 unfolded and was then inoculated (Fig. 3c, right). After 3 d again, the inoculated leaf
461 showed a large SA accumulation in both water- and ASM-treated plants, while the
462 proximal leaf maintained a basal SA level (Fig. 3c). Transient (24-h) exposure to heat did
463 not affect SA content in water-treated plants the day of inoculation, and ASM-treated
464 plants tended to show enhanced SA, yet a large variability was observed. Three days after
465 inoculation, SA content in either leaf was not affected by the prior temperature treatment.
466 The conjugates SA glucoside (SAG) and SA glucose ester (SGE) essentially showed the
467 same variations as SA (Fig. 3d and e). Thus, there was no apparent link between leaf SA
468 content and ASM-induced protection.

469

470 *High temperature does not prevent ASM-induction of defense markers*

471

472 Our results on apple plants contrast with the Arabidopsis / *Pseudomonas syringae* model
473 pathosystem, where high temperature enhances plant susceptibility to the bacteria but
474 does not affect ASM-induced protection (Huot *et al.*, 2017). Nonetheless, in Arabidopsis
475 again, exposure to high temperature for 1 d before and after ASM application inhibits
476 ASM-induced expression of defense genes, including *PR1* (Huot *et al.*, 2017). Such
477 inhibition was also observed in rapeseed, tomato and rice (Kim *et al.*, 2022). Thus, high

478 temperature might prevent the transcriptional induction of defense genes by ASM in apple
479 plants, potentially underlying the loss of ASM-induced protection. To check this
480 hypothesis, we measured the expression of 29 marker genes covering a broad range of
481 defense mechanisms, including *PR1* (Dugé de Bernonville *et al.*, 2014; Chavonet *et al.*,
482 2022), on apple seedlings sprayed with ASM or water and exposed to transient heat or
483 not. Three days after ASM/water treatment, we sampled individual young leaves while
484 inoculating with *E. amylovora*, and kept track of whether the corresponding plants
485 remained healthy or turned diseased. Surprisingly, ASM efficiently induced the
486 transcription of defense markers whatever the temperature scenario, some of the genes
487 being even more induced by ASM at high temperature than at control temperature
488 (Fig. 4a). Thus, the transcriptional induction of defense marker genes by ASM was
489 uncoupled from plant protection at high temperature. Moreover, the expression profile of
490 defense markers at time of inoculation did not account for posterior disease symptoms,
491 as no major difference in gene transcription was observed in plants with healthy or
492 diseased fate (Fig. 4a). This suggests that transcriptional up-regulation of defense genes
493 at the infection site is necessary but not sufficient for effective immunity.
494 As translation can be poorly correlated with transcription during immune regulation (Xu et
495 al., 2017), we reasoned that high temperature may impede the translation of ASM-induced
496 transcripts. However, western blots performed on *MdAGG*, *MdPR2* and *MdPR10*, three
497 defense markers that had been previously associated with induced resistance at control
498 temperature (Chavonet *et al.*, 2022), revealed that protein accumulation was consistent
499 with gene expression (Fig. 4b and c). Overall, the loss of ASM efficiency at high
500 temperature was not captured by the variation of well-established defense markers, either
501 at the transcript or protein level.
502
503 *High temperature dampens transcriptomic response to ASM but does not repress global*
504 *defense*
505
506 To explore the broader changes in the transcriptional landscape induced by ASM and high
507 temperature, we performed a microarray analysis at the time of inoculation following a
508 three-day heatwave (Fig. 5a). For this purpose, we took advantage of the 'Golden

509 Delicious' doubled-haploid GDDH13 – the reference, homozygous apple genome
510 (Daccord *et al.*, 2017). We checked in GDDH13 grafted plants that high temperature also
511 induced a loss of ASM efficiency (Fig. S4), which was broadly similar to, yet less severe
512 than, the one observed in the seedlings of the 'Golden Delicious' progeny (Fig. 2b). We
513 identified 3108 genes differentially expressed in at least one comparison (ASM vs. water
514 at a given temperature, or 35°C vs. 21°C for a given ASM or water treatment). Overall,
515 there was no strong transcriptomic effect of the prior heatwave for water-treated plants
516 (Fig. 5b). Comparatively, ASM triggered massive transcriptomic changes, with patterns of
517 up- and down-regulation that were largely conserved at both temperatures, yet the
518 magnitude of these changes compared to their respective water controls was globally
519 dampened at high temperature (Fig. 5b). GSEA analysis showed that ASM triggered
520 global up-regulation in processes such as response to biotic stimulus, response to stress,
521 signal transduction or alcohol metabolism, and down-regulation in processes such as cell
522 division, photosynthesis, lipid metabolism, cell wall organization or response to hormones
523 – at both temperatures (Fig. 6). Interestingly, the functional categories for which up- or
524 down-regulation was most dampened at high temperature were not focused on defense,
525 but on cell division, signal transduction and various metabolic processes (Fig. 6). Overall,
526 ASM induced large transcriptomic regulation that was softened at high temperatures for
527 some biological processes not obviously associated with defense.
528
529 *Dampening of ASM-induced transcriptional regulation at high temperature is partial but*
530 *pervasive*
531
532 To confirm the transcriptional signature of the ASM × temperature interaction, we selected
533 a set of representative genes for further RT-qPCR analyses on independent experiments.
534 For this purpose, we first performed Clustering Affinity Search Technique (CAST) on the
535 expression profiles of the 3108 genes that were differentially expressed in at least one
536 comparison, generating 26 clusters (Fig. S5; Table S1). Among those, five clusters (Fig.
537 7) were highlighted as they were reminiscent of reduced resistance (R) or increased
538 susceptibility (S) upon ASM application at high temperature, consistent with the
539 phenotypes. Two clusters gathered the majority of genes and reflected the previously

540 described global pattern, with an up- (cluster R1, 1130 genes) or down- (cluster S1, 1223
541 genes) regulation by ASM that is more or less dampened by high temperature. Such heat-
542 induced dampening was exacerbated in clusters R2 (187 genes) and S2 (102 genes),
543 respectively. Moreover, cluster R3 grouped 20 genes that were up-regulated by ASM at
544 control temperature but down-regulated by ASM at high temperature (R3). Overall,
545 clusters R1, R2 and R3 may be viewed as reservoirs of "resistance-associated genes"
546 expected to be up-regulated by ASM, while clusters S1 and S2 may contain "susceptibility-
547 associated genes" expected to be down-regulated by ASM – such up- or down-regulation
548 being potentially vulnerable to high temperature, especially in clusters R2, R3 and S2.
549 Supporting this classification, several PR-protein encoding genes were identified within
550 cluster R1, whereas two genes previously implicated in apple susceptibility to *E.*
551 *amylovora* (*DIPM3a* and *DIPM3b*; Meng *et al.*, 2006) were identified within cluster S1
552 (Table S1).
553
554 We selected 44 genes based on their distribution within these clusters and their functional
555 annotation, including genes putatively involved in defense processes, but also in
556 metabolism, cell cycle, transcription regulation, hormonal synthesis or cell wall properties
557 (Table S2). We designed primers that targeted these genes and also potentially their
558 homologues that were occasionally found across multiple clusters. As controls, we added
559 the three defense genes known for their strong up-regulation by ASM and monitored
560 previously: *MdAGG*, *MdPR2* and *MdPR10*. We then performed qPCR analyses that
561 globally confirmed the expected expression patterns, with a large effect of ASM and a
562 smaller effect of temperature (Fig. 8a). Consistent with this view, a PCA clearly separated
563 the genes based on their belonging to different cluster types ("resistance-associated" *vs*.
564 "susceptibility-associated"), and highlighted the major effect of ASM on gene expression
565 (Fig. 8b). While only a few genes showed significant ASM × temperature interaction (Fig.
566 8a), whereby high temperature restricts the up- or down-regulation induced by ASM, the
567 global interaction was evident on the PCA (Fig. 8b). This analysis confirms the partial but
568 broad-spectrum erosion, at high temperature, of ASM efficiency for transcription
569 regulation.
570

571 *Transcription regulation by ASM is more vulnerable to posterior heatwaves*

572

573 To further assess the vulnerability of ASM-induced transcriptional regulation to high
574 temperature, we varied the number of days (1 to 4) of plant exposure to heatwave, and
575 selected a subset of contrasting genes for qPCR analysis. The patterns of heat application
576 were designed so that i) ASM or water treatments were always applied at the beginning
577 of the last day of heatwaves, and ii) leaves were harvested at the same calendar time, 3 d
578 after the ASM/water treatment (Fig. 9a). The 3-d heatwave corresponded to the same
579 thermal regime as in the previous experiment, and the associated water treatment was
580 therefore selected for data calibration. Overall, the effect of ASM was larger than that of
581 the heatwave duration, and their interaction was minor (Fig. 9b). There was no obvious
582 dose-effect of the duration, which was difficult to interpret. Nonetheless, the transcriptional
583 effect of ASM towards "resistance-associated" markers (or away from "susceptibility-
584 associated" markers) was maximal for the 1-d heatwave, while the amplitude of response
585 to ASM was minimal for the 4-d heatwave (Fig. 9c). Thus, prolonged exposure to
586 heatwave tended to increase the vulnerability of ASM-induced transcriptional regulation,
587 yet the markers were not exquisitely sensitive to the heatwave duration when the
588 heatwave was applied before ASM application.

589

590 Finally, we varied the positioning of the heatwave in relation to the ASM application. A 3-
591 d heatwave was imposed just before, during (as in the previous experiments) or just after
592 the treatment application. Again, all leaves were harvested at the same calendar time, 3
593 d after the ASM/water treatment (Fig. 10a). Gene up- or down-regulation by ASM was
594 more effective when the heatwave occurred before ASM application, and less effective
595 when it occurred afterward, as confirmed by significant interaction between ASM and
596 positioning (Fig. 10b) that was also evident in the PCA (Fig. 10c). These results suggest
597 that high temperature does not prime apple plants towards the erosion of ASM efficiency,
598 but prevents ASM from mounting its full transcriptional regulation straight away.

599

600

601 **Discussion**

602

603 Heatwaves are expected to become more prevalent with climate change and this may
604 affect plant immunity and pathogen virulence, with positive or negative impacts on disease
605 outcome depending on the pathosystem and the thermal scenario (Velásquez *et al.*, 2018;
606 Desaint *et al.*, 2021; Chaloner *et al.*, 2021; Roussin-Léveillée *et al.*, 2024). Here, we found
607 that subjecting apple plants to a short heatwave prior to infection with the bacteria *E.*
608 *amylovora* or the fungus *V. inaequalis* does not impact the development of disease
609 symptoms, but prevents ASM to drive an effective protection despite early accumulation
610 of acibenzolar and active SA metabolism. Our results suggest that pre-exposure to high
611 temperature affects ASM-induced immunity in apple plants, by preventing ASM from fully
612 regulating a wide array of genes that are not solely related to defense.

613

614 Upon high temperature exposure during the ASM application period, apple plants showed
615 an erosion of ASM protection efficiency that covaried with a global dampening of
616 transcriptional regulation. Recent breakthroughs established on the Arabidopsis / *P.*
617 *syringae* model have highlighted that a temperature-susceptible module, that normally
618 drives the accumulation of SA and PR1 defense protein, underpins the loss of immunity
619 at high temperature. However, NPR1-mediated signaling is well-initiated by ASM and
620 other gene modules are still activated to drive effective resistance under these conditions
621 (Huot *et al.*, 2017; Kim *et al.*, 2022). In apple plants, we did not identify a major module
622 vulnerable to high temperature, but rather found that ASM-induced gene regulation was
623 globally less efficient following exposure to high temperature. ASM normally rewires gene
624 transcription so that defense responses are up-regulated while growth-associated
625 processes are down-regulated (Huot *et al.*, 2017; Warneys *et al.*, 2018), which we
626 confirmed here. At high temperature, ASM triggered changes in the transcriptome that
627 were essentially similar to the ones at control temperature, yet attenuated. Overall, plants
628 exposed to high temperature and treated with ASM showed a transcriptomic signature
629 evocative of lower defense and higher susceptibility compared to ASM-treated plants at
630 control temperature (Fig. 11).

631

632 The mechanisms by which high temperature eventually suppresses ASM-induced
633 protection in apple plants may therefore involve many end-players that each partly
634 contributes to plant resistance or susceptibility, rather than a narrow range of defenses
635 controlled by a major thermo-sensitive module of the SA pathway. For instance, heat
636 stress partially impaired ASM-induction of downstream resistance end-players with
637 established roles against different pests. These included e.g. *PR-10* (*PATHOGENESIS*
638 *RELATED-10*), homologues of ribonuclease proteins that possess antimicrobial
639 properties (Liu & Ekramoddoullah, 2006); *BIS2* (*BIPHENYL SYNTHASE 2*), enzymes
640 involved in biosynthesis of biphenyl and dibenzofuran phytoalexins in apple shoots, with
641 antimicrobial activity against *E. amylovora* (Chizzali *et al.*, 2012) and *V. inaequalis*
642 (Hrazdina *et al.*, 1997); or *TPS4* (*TERPENE SYNTHASE 4*), enzymes that participate in
643 the synthesis of defensive volatile compounds in apple (Nieuwenhuizen *et al.*, 2013) such
644 as (*E*,*E*)-$\alpha$-farnesene, a sesquiterpene repellent against rosy apple aphid (*Dysaphis*
645 *plantaginea*; Warneys *et al.*, 2018). Thus, ASM-induced resistance was transcriptionally
646 compromised by heat, correlating here with a loss of protection against *E. amylovora* and
647 *V. inaequalis*.
648
649 Conversely, ASM may normally repress susceptibility or *S* genes that facilitate
650 compatibility with the pathogen, and fails to do so after heat stress, resulting in enhanced
651 plant susceptibility. Only a handful of susceptibility genes are known for the apple / *E.*
652 *amylovora* pathosystem, encoding apple proteins that interact with primary pathogenicity
653 effectors (Campa *et al.*, 2019; Pompili *et al.*, 2020; Tegtmeier *et al.*, 2020), while none
654 have been formally described for *V. inaequalis* so far. Our transcriptomic results support
655 the view that heat stress dampens ASM-driven down-regulation of some of these *S* genes.
656 Further *S* genes likely remain to be discovered, including those related to host physiology
657 that may be required to allow sustained compatibility, as exemplified in other
658 pathosystems (van Schie & Takken, 2014). While our “susceptibility-associated” markers
659 cannot be defined as genuine *S* genes, their de-repression upon heat may enhance plant
660 susceptibility. These markers contained a number of genes plausibly associated with DNA
661 replication or integrity – based on their Arabidopsis homologs (i.e. *WEE1*, *RPA70*, *TK*,
662 *BRCA2*, *ATXR6* – see Table S2 for full gene names). Other markers were possibly linked

663 to cell wall properties (*FLA12*; MacMillan *et al.*, 2010), solute transport (*ENODL17*;
664 Denancé *et al.*, 2014), or cell death execution (*PLP9*; La Camera *et al.*, 2005, 2009),
665 providing a diversity of potential entries whereby pathogens may divert host physiology.
666 In this framework, the erosion of ASM-induced down-regulation of genes useful to plant
667 physiology under heat, combined with the reduced induction of defense mechanisms,
668 would be exploited by the pathogen – effectively leveraging both sides of the "growth–
669 defense tradeoff" (Huot *et al.*, 2014; Monson *et al.*, 2022).
670
671 High temperature seems therefore to directly impede the transcriptional responses to
672 ASM. In line with this idea, the dampened transcriptional pattern was exacerbated when
673 positioning a 3-d heatwave just after the ASM treatment, i.e. when ASM-induced
674 transcription is fully active (Warneys *et al.*, 2018; Chavonet *et al.*, 2022). The molecular
675 mechanisms that link high-temperature perception to transcriptional regulation are
676 increasingly well-described, with the recent discovery of several plant thermosensors
677 (Casal *et al.*, 2024). Interestingly, the thermosensor THERMO-WITH ABA-RESPONSE 1
678 (TWA1) is a predicted intrinsically disordered protein that changes its conformation upon
679 high temperature, allowing physical interaction with the JASMONATE-ASSOCIATED
680 MYC2–LIKE 2 (JAM2) transcription factor and the TOPLESS (TPL) transcriptional
681 repressor, which down-regulates the expression of target genes and optimizes heat stress
682 response (Bohn *et al.*, 2024). JAM2 is a negative regulator of JA signaling (Sasaki-
683 Sekimoto *et al.*, 2013), a hormonal pathway that is down-regulated by *E. amylovora* during
684 the infection of susceptible apple plants (Dugé de Bernonville *et al.*, 2012). Moreover, it
685 has been put forward that the classical JA–SA antagonism in Arabidopsis may turn into
686 synergism under warm conditions (Roussin-Léveillée *et al.*, 2024), due to a tunable
687 regulation loop in the expression of SA biosynthesis genes by JA (Mine *et al.*, 2017). This
688 illustrates potential connections between high temperature sensing and response to biotic
689 cues through transcriptional regulation. It should be stressed, however, that dampening
690 of transcriptional regulation was far from complete, suggesting that the loss of ASM-
691 induced protection at high temperature involves additional layers of biological
692 modifications that are not fully captured by transcripts. The rapid accumulation of
693 acibenzolar acid and the elevated concentrations of salicylates in ASM-treated plants

694 exposed to high temperature suggest that transient heat may exert strong influence on
695 metabolic pathways. Tracking ASM-induced changes in phytohormone contents and in
696 the metabolome upon high temperature could improve our understanding of the
697 mechanisms underlying the loss of protection we report.
698
699 In conclusion, our study unveils a loss of ASM-induced protection against fire blight and
700 apple scab upon transient exposure to heat stress. It covaries with a pervasive dampening
701 of ASM-induced transcription – and probably further physiological rearrangements – so
702 that high temperature makes ASM-treated plants globally less capable of producing
703 defense-related compounds toxic to microbes, and more prone to accumulate susceptible
704 factors that facilitate microbial colonization. As plant response to ASM involves the
705 regulation of many biological processes beyond defense, the protection efficacy of ASM
706 is shaped by the environment due to the interplay between defense and physiology in
707 plants. Disentangling this relationship would enhance our basic understanding of plant
708 immunity in a changing climate, and may offer prospects for stabilizing the efficacy of plant
709 resistance inducers in the field.
710
711
712 **Acknowledgments**
713
714 We thank Anthony Juillard, Brice Marolleau and Mylène Ruh for their involvement in
715 disease assessment assays, the platforms ANAN (analysis of nucleic acids), PHYTO
716 (Phytochemical analyses) and PHENOTIC (Angers Plant Phenotyping Facility,
717 https://doi.org/10.17180/YKBZ-2V85) of the SFR QUASAV for excellent technical
718 assistance, and the UE Horti (https://doi.org/10.15454/1.5573931618268674E12) for the
719 supply of scions. This research was conducted in the framework of i) the regional program
720 “Objectif Végétal, Research, Education and Innovation in Pays de la Loire”, supported by
721 the French Region Pays de la Loire, Angers Loire Métropole and the European Regional
722 Development Fund, ii) the France Agrimer Connaissances Program managed by the
723 French Ministry of Agriculture (Project FAM-Connaissances 2023-11429220-OCASE)
724 and iii) the French Priority Research Programme "Cultiver et Protéger Autrement" (PPR-

CPA) managed by the Agence Nationale de la Recherche (project ANR-20-PCPA-0003 CapZeroPhyto). This work was also supported by the Czech Science Foundation (GACR) project No. 22-17435S, and by grants from the Ministère de l'Education Nationale, de l'Enseignement Supérieur et de la Recherche, France (to E.C.) and from INRAE-AGROECOSYSTEM Department and the Region Pays de la Loire, France (to B-h.N.). B-h.N. received a travel grant from VAAME Doctoral School for a stay in the Laboratory of Growth Regulators.

## Competing interests

None declared.

## Author contributions

A.D., F.P., M.G., R.L. and M.-N.B. conceived the project and designed the research plan. E.C. and B.-h.N. performed most of the experiments, with the contribution of R.C. and C.H. for some experiments. J. Š. and O.N. supervised hormonal analyses. A.D., F.P., M.G., R.L., M.-N.B., E.C. and B.-h.N. analyzed the data and wrote the manuscript. All authors read and approved the final manuscript.

## Data availability

The microarray data sets presented in this study can be found in online repositories. The names of the repository and accession number can be found at: https://www.ncbi.nlm.nih.gov/geo/query/acc.cgi?acc=GSE280234.

## References

**Aćimović SG, Zeng Q, McGhee GC, Sundin GW, Wise JC**. **2015**. Control of fire blight (*Erwinia amylovora*) on apple trees with trunk-injected plant resistance inducers and antibiotics and assessment of induction of pathogenesis-related protein genes. *Frontiers in Plant Science* **6**: 16.

**Ben-Dor A, Shamir R, Yakhini Z**. **1999**. Clustering gene expression patterns. *Journal of Computational Biology* **6**: 281–297.

**Bohn L, Huang J, Weidig S, Yang Z, Heidersberger C, Genty B, Falter-Braun P, Christmann A, Grill E**. **2024**. The temperature sensor TWA1 is required for thermotolerance in *Arabidopsis*. *Nature* **629**: 1126–1132.

**Bowen JK, Mesarich CH, Bus VGM, Beresford RM, Plummer KM, Templeton MD**. **2011**. *Venturia inaequalis*: the causal agent of apple scab. *Molecular Plant Pathology* **12**: 105–122.

**Brisset M-N, Cesbron S, Thomson SV, Paulin J-P**. **2000**. Acibenzolar-S-methyl induces the accumulation of defense-related enzymes in apple and protects from fire blight. *European Journal of Plant Pathology* **106**: 529–536.

**Campa M, Piazza S, Righetti L, Oh C-S, Conterno L, Borejsza-Wysocka E, Nagamangala KC, Beer SV, Aldwinckle HS, Malnoy M**. **2019**. *HIPM* is a susceptibility gene of *Malus* spp.: Reduced expression reduces susceptibility to *Erwinia amylovora*. *Molecular Plant-Microbe Interactions* **32**: 167–175.

**Canet JV, Dobón A, Ibáñez F, Perales L, Tornero P**. **2010a**. Resistance and biomass in Arabidopsis: a new model for Salicylic Acid perception. *Plant Biotechnology Journal* **8**: 126–141.

**Canet JV, Dobón A, Roig A, Tornero P**. **2010b**. Structure-function analysis of *npr1* alleles in Arabidopsis reveals a role for its paralogs in the perception of salicylic acid. *Plant, Cell & Environment* **33**: 1911–1922.

**Casal JJ, Murcia G, Bianchimano L**. **2024**. Plant thermosensors. *Annual Review of Genetics* **58**: 135–158.

**Celton J-M, Gaillard S, Bruneau M, Pelletier S, Aubourg S, Martin-Magniette M-L, Navarro L, Laurens F, Renou J-P**. **2014**. Widespread anti-sense transcription in apple is correlated with siRNA production and indicates a large potential for transcriptional and/or post-transcriptional control. *New Phytologist* **203**: 287–299.

**Chaloner TM, Gurr SJ, Bebber DP**. **2021**. Plant pathogen infection risk tracks global crop yields under climate change. *Nature Climate Change* **11**: 710–715.

**Chavonet E, Gaucher M, Warneys R, Bodelot A, Heintz C, Juillard A, Cournol R, Widmalm G, Bowen JK, Hamiaux C, *et al.* 2022**. Search for host defense markers uncovers an apple agglutination factor corresponding with fire blight resistance. *Plant Physiology* **188**: 1350–1368.

**Cheng C, Gao X, Feng B, Sheen J, Shan L, He P**. **2013**. Plant immune response to pathogens differs with changing temperatures. *Nature Communications* **4**: 2530.

**Chizzali C, Gaid MM, Belkheir AK, Hänsch R, Richter K, Flachowsky H, Peil A, Hanke M-V, Liu B, Beerhues L**. **2012**. Differential expression of biphenyl synthase gene family members in fire-blight-infected apple 'Holsteiner Cox'. *Plant Physiology* **158**: 864–875.

**Coupel-Ledru A, Westgeest AJ, Albasha R, Millan M, Pallas B, Doligez A, Flutre T, Segura V, This P, Torregrosa L, *et al.* 2024**. Clusters of grapevine genes for a burning world. *New Phytologist* **242**: 10–18.

**Daccord N, Celton J-M, Linsmith G, Becker C, Choisne N, Schijlen E, van de Geest H, Bianco L, Micheletti D, Velasco R, *et al.* 2017**. High-quality *de novo* assembly of the apple genome and methylome dynamics of early fruit development. *Nature Genetics* **49**: 1099–1106.

**Denancé N, Szurek B, Noël LD**. **2014**. Emerging functions of nodulin-like proteins in non-nodulating plant species. *Plant and Cell Physiology* **55**: 469–474.

**Desaint H, Aoun N, Deslandes L, Vailleau F, Roux F, Berthomé R**. **2021**. Fight hard or die trying: when plants face pathogens under heat stress. *New Phytologist* **229**: 712–734.

**Ding Y, Sun T, Ao K, Peng Y, Zhang Y, Li X, Zhang Y**. **2018**. Opposite roles of salicylic acid receptors NPR1 and NPR3/NPR4 in transcriptional regulation of plant immunity. *Cell* **173**: 1454-1467.e15.

**Dugé de Bernonville T, Gaucher M, Flors V, Gaillard S, Paulin J-P, Dat JF, Brisset M-N**. **2012**. T3SS-dependent differential modulations of the jasmonic acid pathway in susceptible and resistant genotypes of *Malus* spp. challenged with *Erwinia amylovora*. *Plant Science* **188–189**: 1–9.

**Dugé de Bernonville T, Marolleau B, Staub J, Gaucher M, Brisset M-N**. **2014**. Using molecular tools to decipher the complex world of plant resistance inducers: an apple case study. *Journal of Agricultural and Food Chemistry* **62**: 11403–11411.

**Eckardt NA**. **2002**. Plant disease susceptibility genes? *The Plant Cell* **14**: 1983–1986.

**Floková K, Tarkowská D, Miersch O, Strnad M, Wasternack C, Novák O**. **2014**. UHPLC–MS/MS based target profiling of stress-induced phytohormones. *Phytochemistry* **105**: 147–157.

**Friedrich L, Lawton K, Ruess W, Masner P, Specker N, Gut Rella M, Meier B, Dincher S, Staub T, Uknes S, *et al.* 1996**. A benzothiadiazole derivative induces systemic acquired resistance in tobacco. *The Plant Journal* **10**: 61–70.

**Gessler C, Patocchi A, Sansavini S, Tartarini S, Gianfranceschi L**. **2006**. *Venturia inaequalis* resistance in apple. *Critical Reviews in Plant Sciences* **25**: 473–503.

**Görlach J, Volrath S, Knauf-Beiter G, Hengy G, Beckhove U, Kogel K-H, Oostendorp M, Staub T, Ward E, Kessmann H, *et al.* 1996**. Benzothiadiazole, a novel class of inducers of systemic acquired resistance, activates gene expression and disease resistance in wheat. *The Plant Cell* **8**: 629–643.

**Gorshkov V, Tsers I**. **2022**. Plant susceptible responses: the underestimated side of plant–pathogen interactions. *Biological Reviews* **97**: 45–66.

**Gu Z**. **2022**. Complex heatmap visualization. *iMeta* **1**: e43.

**Guillaumès J, Chevalier M, Parisi L**. **1995**. Étude des relations *Venturia inaequalis* — *Malus* × *domestica* sur vitroplants. *Revue Canadienne de Phytopathologie* **17**: 305–311.

**Holb IJ**. **2007**. Classification of apple cultivar reactions to scab in integrated and organic production systems. *Canadian Journal of Plant Pathology* **29**: 251–260.

**Hrazdina G, Borejsza-Wysocki W, Lester C**. **1997**. Phytoalexin production in an apple cultivar resistant to *Venturia inaequalis*. *Phytopathology* **87**: 868–876.

**Hung J-H, Yang T-H, Hu Z, Weng Z, DeLisi C**. **2012**. Gene set enrichment analysis: performance evaluation and usage guidelines. *Briefings in Bioinformatics* **13**: 281–291.

**Huot B, Castroverde CDM, Velásquez AC, Hubbard E, Pulman JA, Yao J, Childs KL, Tsuda K, Montgomery BL, He SY**. **2017**. Dual impact of elevated temperature on plant defence and bacterial virulence in *Arabidopsis*. *Nature Communications* **8**: 1808.

**Huot B, Yao J, Montgomery BL, He SY**. **2014**. Growth–defense tradeoffs in plants: a balancing act to optimize fitness. *Molecular Plant* **7**: 1267–1287.

**Kassambara A**. **2023a**. rstatix: Pipe-friendly framework for basic statistical tests. R package version 0.7.2.

**Kassambara A**. **2023b**. ggpubr: 'ggplot2' based publication ready plots. R package version 0.6.0.

**Kassambara A, Mundt F**. **2020**. factoextra: Extract and visualize the results of multivariate data analyses. R package version 1.0.7.

**Kim JH, Castroverde CDM, Huang S, Li C, Hilleary R, Seroka A, Sohrabi R, Medina-Yerena D, Huot B, Wang J, *et al.* 2022**. Increasing the resilience of plant immunity to a warming climate. *Nature* **607**: 339–344.

**King EO, Ward MK, Raney DE**. **1954**. Two simple media for the demonstration of pyocyanin and fluorescin. *Journal of Laboratory and Clinical Medicine* **44**: 301–307.

**Kostick SA, Norelli JL, Evans KM**. **2019**. Novel metrics to classify fire blight resistance of 94 apple cultivars. *Plant Pathology* **68**: 985–996.

**Kuźniak E, Głowacki R, Chwatko G, Kopczewski T, Wielanek M, Gajewska E, Skłodowska M**. **2014**. Involvement of ascorbate, glutathione, protein S-thiolation and salicylic acid in benzothiadiazole-inducible defence response of cucumber against *Pseudomonas syringae* pv *lachrymans*. *Physiological and Molecular Plant Pathology* **86**: 89–97.

**La Camera S, Balagué C, Göbel C, Geoffroy P, Legrand M, Feussner I, Roby D, Heitz T**. **2009**. The *Arabidopsis* patatin-like protein 2 (PLP2) plays an essential role in cell death execution and differentially affects biosynthesis of oxylipins and resistance to pathogens. *Molecular Plant-Microbe Interactions* **22**: 469–481.

**La Camera S, Geoffroy P, Samaha H, Ndiaye A, Rahim G, Legrand M, Heitz T**. **2005**. A pathogen-inducible patatin-like lipid acyl hydrolase facilitates fungal and bacterial host colonization in Arabidopsis. *The Plant Journal* **44**: 810–825.

**Lawton KA, Friedrich L, Hunt M, Weymann K, Delaney T, Kessmann H, Staub T, Ryals J**. **1996**. Benzothiadiazole induces disease resistance in *Arabidopsis* by activation of the systemic acquired resistance signal transduction pathway. *The Plant Journal* **10**: 71–82.

**Lê S, Josse J, Husson F**. **2008**. FactoMineR: An R package for multivariate analysis. *Journal of Statistical Software* **25**: 1–18.

**Liu J-J, Ekramoddoullah AKM**. **2006**. The family 10 of plant pathogenesis-related proteins: Their structure, regulation, and function in response to biotic and abiotic stresses. *Physiological and Molecular Plant Pathology* **68**: 3–13.

**Long SP, Ort DR**. **2010**. More than taking the heat: crops and global change. *Current Opinion in Plant Biology* **13**: 240–247.

**MacMillan CP, Mansfield SD, Stachurski ZH, Evans R, Southerton SG**. **2010**. Fasciclin-like arabinogalactan proteins: specialization for stem biomechanics and cell wall architecture in Arabidopsis and *Eucalyptus*. *The Plant Journal* **62**: 689–703.

871 **Malamy J, Hennig J, Klessig DF**. **1992**. Temperature-dependent induction of salicylic acid and its
872 conjugates during the resistance response to tobacco mosaic virus infection. *The Plant Cell* **4**: 359–366.

873 **Mangiafico SS**. **2024**. rcompanion: Functions to support extension education program evaluation. R
874 package version 2.4.36.

875 **Marchin RM, Backes D, Ossola A, Leishman MR, Tjoelker MG, Ellsworth DS**. **2022**. Extreme heat
876 increases stomatal conductance and drought-induced mortality risk in vulnerable plant species. *Global*
877 *Change Biology* **28**: 1133–1146.

878 **Marolleau B, Gaucher M, Heintz C, Degrave A, Warneys R, Orain G, Lemarquand A, Brisset M-N**.
879 **2017**. When a plant resistance inducer leaves the lab for the field: integrating ASM into routine apple
880 protection practices. *Frontiers in Plant Science* **8**: 1938.

881 **Maxson-Stein K, He S-Y, Hammerschmidt R, Jones AL**. **2002**. Effect of treating apple trees with
882 acibenzolar-*S*-methyl on fire blight and expression of pathogenesis-related protein genes. *Plant Disease*
883 **86**: 785–790.

884 **Meng X, Bonasera JM, Kim JF, Nissinen RM, Beer SV**. **2006**. Apple proteins that interact with DspA/E, a
885 pathogenicity effector of *Erwinia amylovora*, the fire blight pathogen. *Molecular Plant-Microbe Interactions*
886 **19**: 53–61.

887 **Mine A, Nobori T, Salazar-Rondon MC, Winkelmüller TM, Anver S, Becker D, Tsuda K**. **2017**. An
888 incoherent feed-forward loop mediates robustness and tunability in a plant immune network. *EMBO Reports*
889 **18**: 464–476.

890 **Monson RK, Trowbridge AM, Lindroth RL, Lerdau MT**. **2022**. Coordinated resource allocation to plant
891 growth–defense tradeoffs. *New Phytologist* **233**: 1051–1066.

892 **Nieuwenhuizen NJ, Green SA, Chen X, Bailleul EJD, Matich AJ, Wang MY, Atkinson RG**. **2013**.
893 Functional genomics reveals that a compact terpene synthase gene family can account for terpene volatile
894 production in apple. *Plant Physiology* **161**: 787–804.

895 **Parent B, Turc O, Gibon Y, Stitt M, Tardieu F**. **2010**. Modelling temperature-compensated physiological
896 rates, based on the co-ordination of responses to temperature of developmental processes. *Journal of*
897 *Experimental Botany* **61**: 2057–2069.

898 **Paulin J-P, Sampson R**. **1973**. Le feu bactérien en France. II. Caractères des souches d'*Erwinia amylovora*
899 (Burrill), Winslow et al. 1920, isolées du foyer franco-belge. *Annales de Phytopathologie* **5**: 389–397.

900 **Peng Y, Yang J, Li X, Zhang Y**. **2021**. Salicylic acid: biosynthesis and signaling. *Annual Review of Plant*
901 *Biology* **72**: 761–791.

902 **Perrin A, Daccord N, Roquis D, Celton J-M, Vergne E, Bucher E**. **2020**. Divergent DNA methylation
903 signatures of juvenile seedlings, grafts and adult apple trees. *Epigenomes* **4**: 4.

904 **Pompili V, Dalla Costa L, Piazza S, Pindo M, Malnoy M**. **2020**. Reduced fire blight susceptibility in apple
905 cultivars using a high-efficiency CRISPR/Cas9-FLP/FRT-based gene editing system. *Plant Biotechnology*
906 *Journal* **18**: 845–858.

907 **Qiu J, Xie J, Chen Y, Shen Z, Shi H, Naqvi NI, Qian Q, Liang Y, Kou Y**. **2022**. Warm temperature
908 compromises JA-regulated basal resistance to enhance *Magnaporthe oryzae* infection in rice. *Molecular*
909 *Plant* **15**: 723–739.

910 **Quint M, Delker C, Franklin KA, Wigge PA, Halliday KJ, Zanten M van**. **2016**. Molecular and genetic
911 control of plant thermomorphogenesis. *Nature Plants* **2**: 15190.

912 **R Development Core Team**. **2022**. R: A language and environment for statistical computing.

913 **R Studio Team**. **2024**. RStudio: Integrated development environment for R.

914 **Ratchaseema MTN, Kladsuwan L, Soulard L, Swangmaneecharern P, Punpee P, Klomsa-ard P,**
915 **Sriroth K, Keawsompong S**. **2021**. The role of salicylic acid and benzothiadiazole in decreasing
916 phytoplasma titer of sugarcane white leaf disease. *Scientific Reports* **11**: 15211.

917 **Richard MMS, Knip M, Aalders T, Beijaert MS, Takken FLW**. **2020**. Unlike many disease resistances,
918 Rx1-mediated immunity to Potato Virus X is not compromised at elevated temperatures. *Frontiers in*
919 *Genetics* **11**: 417.

920 **Roussin-Léveillée C, Rossi CAM, Castroverde CDM, Moffett P**. **2024**. The plant disease triangle facing
921 climate change: a molecular perspective. *Trends in Plant Science* **29**: 895–914.

922 **Saeed AI, Sharov V, White J, Li J, Liang W, Bhagabati N, Braisted J, Klapa M, Currier T, Thiagarajan**
923 **M, *et al.* 2003**. TM4: A free, open-source system for microarray data management and analysis.
924 *BioTechniques* **34**: 374–378.

925 **Sandroni M, Liljeroth E, Mulugeta T, Alexandersson E**. **2020**. Plant resistance inducers (PRIs):
926 perspectives for future disease management in the field. *CABI Reviews* **15**: 001.

927 **Sasaki-Sekimoto Y, Jikumaru Y, Obayashi T, Saito H, Masuda S, Kamiya Y, Ohta H, Shirasu K**. **2013**.
928 Basic helix-loop-helix transcription factors JASMONATE-ASSOCIATED MYC2-LIKE1 (JAM1), JAM2, and
929 JAM3 are negative regulators of jasmonate responses in Arabidopsis. *Plant Physiology* **163**: 291–304.

930 **van Schie CCN, Takken FLW**. **2014**. Susceptibility genes 101: how to be a good host. *Annual Review of*
931 *Phytopathology* **52**: 551–581.

932 **Schmittgen TD, Livak KJ**. **2008**. Analyzing real-time PCR data by the comparative $C_T$ method. *Nature*
933 *Protocols* **3**: 1101–1108.

934 **Shields A, Yao L, Kim JH, Al-Timmen WMA, Li S, Marchetta EJR, Shivnauth V, Chen T, He SY, Xin X,**
935 ***et al.* 2023**. Warm temperature suppresses plant systemic acquired resistance by intercepting the *N*-
936 hydroxypipecolic acid immune pathway. : 2023.10.31.564368.

937 **Široká J, Brunoni F, Pěnčík A, Mik V, Žukauskaitė A, Strnad M, Novák O, Floková K**. **2022**. High-
938 throughput interspecies profiling of acidic plant hormones using miniaturised sample processing. *Plant*
939 *Methods* **18**: 122.

940 **Smyth GK**. **2005**. limma: Linear models for microarray data. In: Gentleman R, Carey VJ, Huber W, Irizarry
941 RA, Dudoit S, eds. Bioinformatics and Computational Biology Solutions Using R and Bioconductor. New
942 York, USA: Springer, 397–420.

943 **Stevens RB**. **1960**. Chapter 10 - Cultural practices in disease control. In: Horsfall JG, Dimond AE, eds.
944 Plant Pathology: An Advanced Treatise. New York and London: Academic Press, 357–429.

945 **Subramanian A, Tamayo P, Mootha VK, Mukherjee S, Ebert BL, Gillette MA, Paulovich A, Pomeroy**
946 **SL, Golub TR, Lander ES, *et al.* 2005**. Gene set enrichment analysis: A knowledge-based approach for
947 interpreting genome-wide expression profiles. *Proceedings of the National Academy of Sciences of the*
948 *United States of America* **102**: 15545–15550.

949 **Tegtmeier R, Pompili V, Singh J, Micheletti D, Silva KJP, Malnoy M, Khan A**. **2020**. Candidate gene
950 mapping identifies genomic variations in the fire blight susceptibility genes *HIPM* and *DIPM* across the *Malus*
951 germplasm. *Scientific Reports* **10**: 16317.

952 **Tripathi D, Jiang Y-L, Kumar D**. **2010**. SABP2, a methyl salicylate esterase is required for the systemic
953 acquired resistance induced by acibenzolar-*S*-methyl in plants. *FEBS Letters* **584**: 3458–3463.

954 **Ullah C, Tsai C-J, Unsicker SB, Xue L, Reichelt M, Gershenzon J, Hammerbacher A**. **2019**. Salicylic
955 acid activates poplar defense against the biotrophic rust fungus *Melampsora larici-populina* via increased
956 biosynthesis of catechin and proanthocyanidins. *New Phytologist* **221**: 960–975.

957 **Vandesompele J, de Preter K, Pattyn F, Poppe B, van Roy N, de Paepe A, Speleman F**. **2002**. Accurate
958 normalization of real-time quantitative RT-PCR data by geometric averaging of multiple internal control
959 genes. *Genome Biology* **3**: research0034.1-0034.11.

960 **Vanneste JL (Ed.)**. **2000**. *Fire blight: the disease and its causative agent,* Erwinia amylovora. Wallingford,
961 UK: CABI.

962 **Vasseur F, Pantin F, Vile D**. **2011**. Changes in light intensity reveal a major role for carbon balance in
963 *Arabidopsis* responses to high temperature. *Plant, Cell & Environment* **34**: 1563–1576.

964 **Velásquez AC, Castroverde CDM, He SY**. **2018**. Plant–pathogen warfare under changing climate
965 conditions. *Current Biology* **28**: R619–R634.

966 **Walters DR, Ratsep J, Havis ND**. **2013**. Controlling crop diseases using induced resistance: challenges
967 for the future. *Journal of Experimental Botany* **64**: 1263–1280.

968 **Walters D, Walsh D, Newton A, Lyon G**. **2005**. Induced resistance for plant disease control: Maximizing
969 the efficacy of resistance elicitors. *Phytopathology* **95**: 1368–1373.

970 **Warneys R, Gaucher M, Robert P, Aligon S, Anton S, Aubourg S, Barthes N, Braud F, Cournol R,**
971 **Gadenne C, *et al.* 2018**. Acibenzolar-*S*-methyl reprograms apple transcriptome toward resistance to rosy
972 apple aphid. *Frontiers in Plant Science* **9**: 1795.

973 **Wickham H**. **2016**. *ggplot2: Elegant Graphics for Data Analysis*. New York, USA: Springer-Verlag.

974 **Wu T, Hu E, Xu S, Chen M, Guo P, Dai Z, Feng T, Zhou L, Tang W, Zhan L, *et al.* 2021**. clusterProfiler
975 4.0: A universal enrichment tool for interpreting omics data. *The Innovation* **2**: 100141.

976 **Zeng Q, Puławska J, Schachterle J**. **2021**. Early events in fire blight infection and pathogenesis of *Erwinia*
977 *amylovora*. *Journal of Plant Pathology* **103**: 13–24.

978 **Zhang W, Chen S, Abate Z, Nirmala J, Rouse MN, Dubcovsky J**. **2017**. Identification and characterization
979 of *Sr13*, a tetraploid wheat gene that confers resistance to the Ug99 stem rust race group. *Proceedings of*
980 *the National Academy of Sciences of the United States of America* **114**: E9483–E9492.

981 **Zhu Y, Qian W, Hua J**. **2010**. Temperature modulates plant defense responses through NB-LRR proteins.
982 *PLoS Pathogens* **6**: e1000844.

983

984

985 *Supporting Information*

986

987 Additional Supporting Information may be found online in the Supporting Information
988 section at the end of the article.

989

990 **Figure S1.** Climatic variables measured at the meteorological station of Beaucouzé
991 (France) for the eleven hottest days recorded between March 2016 and July 2018.
992 **Figure S2.** Climate dynamics applied in the growth chamber to study the effect of
993 heatwaves on apple response to ASM.
994 **Figure S3.** Impact of heat and treatment on plant phenotype, and representative
995 photographs of apple seedlings and their typical disease symptoms.
996 **Figure S4.** Accumulation of high temperatures prior to inoculation impairs the ability of
997 apple grafts of GDDH13 to mount an effective ASM-induced protection against *E.*
998 *amylovora*.
999 **Figure S5.** Identification of gene clusters by CAST.
1000 **Table S1.** List of genes that are differentially regulated by ASM treatment and transient
1001 heat according to the microarray analysis.
1002 **Table S2.** Design of “resistance” and “susceptibility” marker genes.

1003

1004

1005 **Figures captions**

1006

1007 **Fig. 1. Protection provided by ASM to apple seedlings against *E. amylovora* and *V.***
1008 ***inaequalis* is impaired by transient exposure to heat. (a)** Schematic representation of
1009 the experimental protocol applied to plants for *E. amylovora* (left) and *V. inaequalis* (right)
1010 disease assessment (details in Methods). Air temperature during the contrasting thermal
1011 scenario (period in the growth chamber) is color-coded according to the color map. Arrows
1012 indicate the application of ASM (or water) treatment and pathogen inoculation on the
1013 youngest unfolded leaf. **(b)** Stacked bar chart showing the proportion of healthy
1014 (asymptomatic) and diseased (symptomatic) seedlings inoculated with *E. amylovora*, 21 d
1015 post-inoculation. **(c)** Stacked bar chart showing the proportion of healthy (no visible

1016 sporulation) and diseased (visible sporulation) seedlings inoculated with *V. inaequalis*,
1017 21 d post-inoculation. Data represent 78 to 85 biological replicates from 2 independent
1018 trials for each pathogen (n = total number of plants). Statistical significance was
1019 determined using pairwise Fisher's exact tests; same letters indicate groups that are not
1020 significantly different. Icons created in BioRender.com.
1021
1022 **Fig. 2. Accumulation of high temperatures prior to inoculation impairs the ability of**
1023 **apple seedlings to mount an effective ASM-induced protection against *E.***
1024 ***amylovora*. (a)** Schematic representation of the experimental protocol (details in
1025 Methods). Air temperature during the contrasting thermal scenario (period in the growth
1026 chamber) is color-coded according to the color map. Arrows indicate the application of
1027 ASM (or water) treatment and pathogen inoculation on the youngest unfolded leaf. **(b)**
1028 Stacked bar chart of seedlings showing the proportion of healthy (asymptomatic) and
1029 diseased (symptomatic) seedlings inoculated with *E. amylovora*, 21 d post-inoculation.
1030 Data represent 60 biological replicates from 3 independent trials (n = total number of
1031 plants). Statistical significance was determined using pairwise Fisher's exact tests; same
1032 letters indicate groups that are not significantly different. Icons created in BioRender.com.
1033
1034 **Fig. 3. High temperature does not alter ASM uptake or SA metabolism in apple**
1035 **seedlings. (a)** and **(b)** Content of ASM and acibenzolar acid (biologically-active
1036 catabolite) in the lamina of ASM-treated leaves (n = 10, each pooled from 2 different
1037 plants). Apple seedlings were sprayed with ASM ($t_0$) and immediately transferred into a
1038 chamber at 20°C or 35°C. The youngest fully unfolded leaf (rank N) and the leaf below
1039 (rank N-1) were sampled after 6 h (when the sprayed solution had evaporated) and
1040 thoroughly rinsed before quantification of **(a)** ASM and **(b)** acibenzolar acid. **(c)**, **(d)** and
1041 **(e)** Content of salicylates in the lamina of water- or ASM-treated leaves (n = 6, each pooled
1042 from 8 different plants). Apple seedlings were sprayed with water or ASM ($t_0$) and
1043 immediately transferred into a chamber at 20°C or 35°C for 24 h, before being placed in
1044 a greenhouse. Three days after spraying ($t_0$+3d), half of the plants was sampled for the
1045 youngest fully unfolded leaf at time of spraying (rank N) and the leaf above (rank N+1),
1046 while the other half was inoculated with *E. amylovora* at leaf N+1. At three days post-

1047 inoculation (3 dpi, $t_0$+6d), the inoculated leaf N+1 and leaf N were harvested. A batch of
1048 plants was also harvested for leaf N just before $t_0$, in the greenhouse where the seedlings
1049 were grown. The samples were quantified for **(c)** salicylic acid (SA), **(d)** SA glucoside
1050 (SAG) and **(e)** SA glucose ester (SGE).
1051
1052 **Fig. 4. High temperature does not prevent ASM-induction of defense markers. (a)**
1053 Retrospective transcriptional analysis of 29 marker genes covering a broad range of apple
1054 defense mechanisms. Following a scenario similar as in Fig. 1a, young leaves of apple
1055 seedlings were individually sampled while inoculating with *E. amylovora*, and grouped *a*
1056 *posteriori* depending on the healthy or diseased fate of their corresponding plant.
1057 Heatmaps show relative gene expression and ANOVA effect sizes ($\eta_g^2$) of treatment,
1058 temperature and their interaction, as well as their respective significance level (*P<0.05,
1059 **P<0.01, ***P<0.001, ****P<0.0001), for both types of plants. Expression values of the
1060 average of water-treated leaves from healthy and diseased plants exposed to 20°C were
1061 used for the calculation of the $\log_2$ ratio. Expression values were obtained from 5–9
1062 biological replicates (pools of 2 to 4 youngest unfolded leaves at time of ASM or water
1063 treatment) from a single trial. **(b)** Relative expression of *MdAGG*, *MdPR2* and *MdPR10*
1064 from two independent experiments performed in the same conditions as in Fig. 5a (3-d
1065 heatwave, GDDH13 grafted plants – see afterwards). The youngest unfolded leaf at time
1066 of sampling was collected from 5 plants per experiment. **(c)** Protein immunodetection of
1067 defense-associated proteins. Equal quantities (10 µg) of each protein sample were loaded
1068 and run in three separate SDS-PAGE gels. Following transfer to PVDF membranes, each
1069 blot was probed with the appropriate primary antibody to detect MdAGG, MdPR2, and
1070 MdPR10. Each sample corresponds to a pool of proteins extracted from the 5 biological
1071 replicates per experiment presented in **(b)**.
1072
1073 **Fig. 5. High temperature dampens transcriptomic response to ASM. (a)** Schematic
1074 diagram of the experimental protocol. Air temperature during the contrasting thermal
1075 scenario (period in the growth chamber) is color-coded according to the color map. Arrows
1076 indicate the application of ASM or water treatment and the sampling of the youngest
1077 unfolded leaf of GDDH13 grafted plants dedicated to microarray analysis. **(b)** Heatmap of

1078 3108 DEGs identified in at least one microarray comparison. DEGs were defined by a
1079 $|\log_2 \text{ratio}| \geq 1$ and $P < 0.05$. The hierarchical clustering dendrogram was constructed from
1080 the dissimilarity matrix. Expression values were obtained from 2 biological replicates
1081 (each pooled from the youngest fully expanded leaf of 4 grafted plants) from 2
1082 independent trials.
1083
1084 **Fig. 6. Biological processes affected by high temperature during ASM-induced**
1085 **transcriptomic changes are not focused on defense.** Ridgeline plot of GSEA on
1086 biological process ontology performed on comparison ASM/water for plants exposed to
1087 both 21°C and 35°C and 35°C/21°C comparison for ASM-treated plants. GSEA was
1088 obtained by 10.000 permutations with Benjamini and Hochberg procedure for p-value
1089 adjustment.
1090
1091 **Fig. 7. Identification of "resistance-associated" and "susceptibility-associated"**
1092 **marker genes by clustering.** CAST clustering performed on the 3108 DEGs (Table S1
1093 and Fig. S5) yielded several clusters evocative of resistant (R1, R2 and R3) and
1094 susceptible (S1 and S2) marker genes. The average pattern of expression ratio (± sd) is
1095 shown for each cluster. The number of DEGs in each resistance or susceptibility cluster
1096 are indicated in the upper right- or left-hand corner, respectively. To facilitate the
1097 interpretation of the variations in ratios, barplots showing the inferred expression pattern
1098 relative to the control (water, 21°C) are placed in the lower left- or right-hand corner of
1099 resistance and susceptibility clusters, respectively.
1100
1101 **Fig. 8. High temperature erodes ASM-induced transcriptional regulation of**
1102 **resistance- and susceptibility-associated marker genes.** Expression values of water-
1103 treated leaves from plants exposed to 21°C were used for the calculation of the $\log_2$ ratio.
1104 Expression values were obtained from 10 biological replicates equally from 2 independent
1105 trials. **(a)** Heatmap showing relative gene expression and ANOVA effect sizes ($\eta_g^2$) of
1106 treatment, temperature and their interaction, as well as their respective significance level
1107 (*P<0.05, **P<0.01, ***P<0.001, ****P<0.0001). **(b)** PCA representation of relative gene
1108 expression on the two first dimensions, with the contribution of markers color-coded

1109 according to their cluster (top) and the distribution of samples grouped by treatment and
1110 temperature (bottom). Ellipses correspond to 95% confidence intervals around the
1111 centroid. Note that a single marker may be assigned to several clusters if the
1112 corresponding primer targets several homologous genes (Table S2).
1113
1114 **Fig. 9. The duration of heat exposure before ASM treatment moderately affects the**
1115 **dampening of ASM-induced transcriptional regulation.** Effect of heat duration prior to
1116 treatment on the expression of selected markers 3 d after ASM or water treatment, in
1117 grafted plants subjected to a 1-d, 2-d, 3-d and 4-d heatwave at 35°C. Expression values
1118 of water-treated leaves from plants exposed to 3-d 35°C were used for the calculation of
1119 the $\log_2$ ratio. Expression values were obtained from 6 biological replicates equally from
1120 2 independent trials. **(a)** Schematic diagram of the experimental protocol. Air temperature
1121 during the contrasting thermal scenario (period in the growth chamber) is color-coded
1122 according to the color map. Arrows indicate the application of ASM (or water) treatment
1123 and the sampling of the youngest unfolded leaves. **(b)** Heatmap showing relative gene
1124 expression and ANOVA effect sizes ($\eta_g^2$) of treatment, temperature and their interaction,
1125 as well as their respective significance level (*P<0.05, **P<0.01, ***P<0.001,
1126 ****P<0.0001). **(c)** PCA representation of relative gene expression on the two first
1127 dimensions, with the contribution of markers color-coded according to their cluster (top)
1128 and the distribution of samples grouped by treatment and temperature (bottom). Ellipses
1129 correspond to 95% confidence intervals around the centroid. Note that a single marker
1130 may be assigned to several clusters if the corresponding primer targets several
1131 homologous genes (Table S2).
1132
1133 **Fig. 10. A heatwave posterior to ASM application dampens ASM-induced**
1134 **transcriptional regulation more strongly than a prior heatwave.** Effect of heatwave
1135 positioning on expression of selected markers 3 d after ASM or water treatment, in grafted
1136 plants subjected to a 3-d heatwave at 35°C before, during or after ASM or water treatment.
1137 Expression values of water-treated leaves from plants under heatwave during the
1138 treatment were used for the calculation of the $\log_2$ ratio. Expression values were obtained
1139 from 6 biological replicates equally from 2 independent trials. **(a)** Schematic diagram of

1140 the experimental protocol. Air temperature during the contrasting thermal scenario (period
1141 in the growth chamber) is color-coded according to the color map. Arrows indicate the
1142 application of ASM (or water) treatment and the sampling of the youngest unfolded leaves.
1143 **(b)** Heatmap showing relative gene expression and ANOVA effect sizes ($\eta_g^2$) of treatment,
1144 temperature and their interaction, as well as their respective significance level (*P<0.05,
1145 **P<0.01, ***P<0.001, ****P<0.0001). **(c)** PCA representation of relative gene expression
1146 on the two first dimensions, with the contribution of markers color-coded according to their
1147 cluster (top) and distribution of samples grouped by treatment and temperature (bottom).
1148 Ellipses correspond to 95% confidence intervals around the centroid. Note that a single
1149 marker may be assigned to several clusters if the corresponding primer targets several
1150 homologous genes (Table S2).
1151
1152 **Fig. 11. Working model for the loss of ASM-induced protection of apple plants upon**
1153 **transient heat.** At control temperature (20°C), spraying apple plants with ASM prior to
1154 inoculation with the bacteria *E. amylovora* or the fungus *V. inaequalis* allows apple leaves
1155 to mount an effective transcriptional response whereby resistance-associated genes are
1156 up-regulated and susceptibility-associated genes are down-regulated – which reduces the
1157 incidence of fire blight or apple scab. When a heatwave (35°C) occurs in between ASM
1158 application and pathogen inoculation, ASM-induced transcriptional regulation is
1159 dampened, ultimately enabling pathogens to proliferate. Created in BioRender.com.
1160
1161
1162 **Supplementary figures captions**
1163
1164 **Fig. S1. Climatic variables measured at the meteorological station of Beaucouzé**
1165 **(France) for the eleven hottest days recorded between March 2016 and July 2018.**
1166 Empty circles correspond to individual, hourly values. **(a)** Air temperature, **(b)** relative
1167 humidity (RH), **(c)** solar radiation and corresponding percent irradiance. Grey solid curves
1168 represent the average trend as determined by the non-parametric loess method (span =
1169 0.5), surrounded by the standard error (grey shaded area). Red dashed lines indicate the

1170 piecewise linear approximation of each climatic variable that was used to design the
1171 heatwave scenarios in the growth chamber.
1172
1173 **Fig. S2. Climate dynamics applied in the growth chamber to study the effect of**
1174 **heatwaves on apple response to ASM. (a)** “Control”, **(b)** “Short” and **(c)** “Long”
1175 scenarios showing the daily variations in temperature, relative humidity (RH) and percent
1176 irradiance applied in growth chambers. Combination of these elemental daily programs
1177 were used to reproduce the different thermal scenarios that were studied.
1178
1179 **Fig. S3. Impact of heat and treatment on plant phenotype, and representative**
1180 **photographs of apple seedlings and their typical disease symptoms. (a)**, **(b)**, and **(c)**
1181 Boxplots and jitter plots showing the impact of temperature scenario and ASM or water
1182 treatment on apple seedling phenotypes. All measurements were performed on the same
1183 plants of the same experiment (Methods). At time 0, plants were sprayed with ASM or
1184 water and immediately transferred from a greenhouse to a growth chamber with controlled
1185 environmental conditions. Air temperature was maintained at either 20°C or 35°C for 24
1186 h, and all plants then remained in the growth chamber at 20°C during 48 h more. The
1187 elongation rate of **(a)** the stem and **(b)** the youngest unfolded leaf was calculated using
1188 measurements made before treatment and 3 d after treatment. Statistical differences
1189 between ASM and water treatment were determined at each temperature using pairwise
1190 t-tests adjusted by the Bonferroni method, and were deemed not significant (ns). **(c)**
1191 Stomatal conductance ($g_s$) was measured on the youngest unfolded leaf at time of
1192 ASM/water treatment application (left panel) and on the leaf rank immediately below (right
1193 panel), 1.5 h before treatment and 3, 48 and 72 h after treatment. Multiple mean
1194 comparisons were performed between each combination of both factors at each time point
1195 using pairwise t-tests adjusted by the Bonferroni method (* $0.05 \geq P > 0.01$, **
1196 $0.01 \geq P > 0.001$). Note that non-significant differences have been omitted for clarity. **(d)**
1197 Photograph of a representative batch of apple seedlings at the start of the experiment. **(e)**
1198 Photograph of systemic fire blight necrosis symptoms on a diseased apple seedling, 21 d
1199 after inoculation by *E. amylovora*. The inoculated leaf is indicated by a white arrowhead
1200 and the picture focuses on necrotic symptoms spreading along the midvein of a distant

1201 leaf, and along the stem up to the plant apex. **(f)** Photograph of an apple seedling leaf
1202 showing *V. inaequalis* sporulation, 21 d after inoculation.
1203
1204 **Fig. S4. Accumulation of high temperatures prior to inoculation impairs the ability**
1205 **of apple grafts of GDDH13 to mount an effective ASM-induced protection against *E.***
1206 ***amylovora*. (a)** Schematic representation of the experimental protocol (details in
1207 Methods). Air temperature during the contrasting thermal scenario (period in the growth
1208 chamber) is color-coded according to the color map. Arrows indicate the application of
1209 ASM (or water) treatments and pathogen inoculation on the youngest unfolded leaf. **(b)**
1210 Stacked bar chart showing the proportion of healthy (asymptomatic) and diseased
1211 (symptomatic) grafted plants inoculated with *E. amylovora*, 28 d post-inoculation. Data
1212 represent 48 biological replicates from 4 independent trials (n = total number of plants).
1213 Statistical significance was determined using pairwise Fisher's exact tests; same letters
1214 indicate groups that are not significantly different. Icons created in BioRender.com. **(c)**
1215 Photograph of a diseased GDDH13 graft presenting fire blight symptoms on the apex and
1216 displaying the typical “hook shape”.
1217
1218 **Fig. S5. Identification of gene clusters by CAST.** Clustering was based on the
1219 expression pattern of 3108 genes that displayed differential expression (defined by a $|\log_2$
1220 $\text{ratio}| \geq 1$ and $P < 0.05$ in at least one microarray comparison, see Fig. 5b) in plants treated
1221 with ASM or water and exposed to control (21°C) or elevated (35°C) temperature. Pearson
1222 correlation distance metric (0.95 threshold affinity) allowed the construction of 26 clusters.
1223 Grey lines correspond to the expression ratio pattern of each individual DEG. Red points
1224 correspond to the average $\log_2$ expression ratio (± sd) within each comparison, for each
1225 cluster. The number of DEGs grouped in each cluster and the corresponding cluster
1226 number (and name for R1, R2, R3, S1 and S2 investigated in Fig. 7) are indicated in the
1227 upper right- and left-hand corner of each box, respectively.
1228
1229
1230 **Supplementary tables captions**
1231

1232 **Table S1. List of genes that are differentially regulated by ASM treatment and**
1233 **transient heat according to the microarray analysis.** Differentially expressed genes
1234 were defined by a $|\log_2 \text{ratio}| \geq 1$ and $P < 0.05$. The table shows gene accession, gene
1235 description, gene symbol (if any), $\log_2$ fold change within each comparison, cluster
1236 membership (see Fig. S5), and functional annotation. Gene description and functional
1237 annotation are based on the GDDH13 genome annotation (Daccord *et al.*, 2017).
1238
1239 **Table S2. Design of "resistance" and "susceptibility" marker genes.** Genes initially
1240 selected through CAST belonged to "resistance" (R1, R2, R3) or "susceptibility" (S1, S2)
1241 clusters (Fig. 7). Homologous genes were searched in the genome, and were eventually
1242 found in the same or an alternative cluster. Primers were designed to target as many
1243 homologous genes as possible, and the targeted ones are bolded. The table shows gene
1244 name, functional annotation, accession, cluster membership (if any), and primer sequence
1245 and concentration. Functional annotation is based on the GDDH13 genome annotation
1246 (Daccord *et al.*, 2017).

Figure 1

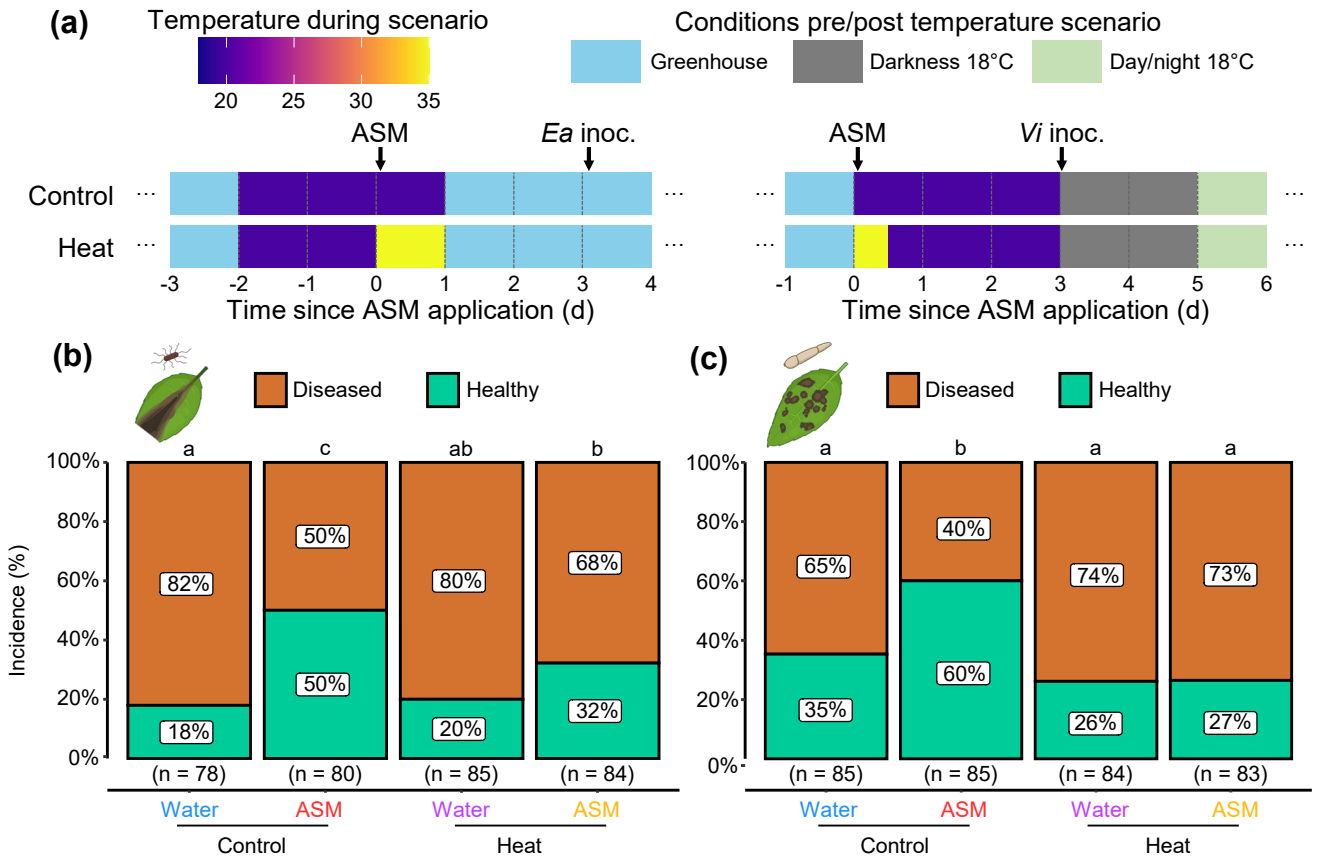


**Fig. 1. Protection provided by ASM to apple seedlings against *E. amylovora* and *V. inaequalis* is impaired by transient exposure to heat. (a)** Schematic representation of the experimental protocol applied to plants for *E. amylovora* (left) and *V. inaequalis* (right) disease assessment (details in Methods). Air temperature during the contrasting thermal scenario (period in the growth chamber) is color-coded according to the color map. Arrows indicate the application of ASM (or water) treatment and pathogen inoculation on the youngest unfolded leaf. **(b)** Stacked bar chart showing the proportion of healthy (asymptomatic) and diseased (symptomatic) seedlings inoculated with *E. amylovora*, 21 d post-inoculation. **(c)** Stacked bar chart showing the proportion of healthy (no visible sporulation) and diseased (visible sporulation) seedlings inoculated with *V. inaequalis*, 21 d post-inoculation. Data represent 78 to 85 biological replicates from 2 independent trials for each pathogen (n = total number of plants). Statistical significance was determined using pairwise Fisher's exact tests; same letters indicate groups that are not significantly different. Icons created in BioRender.com.

Figure 2

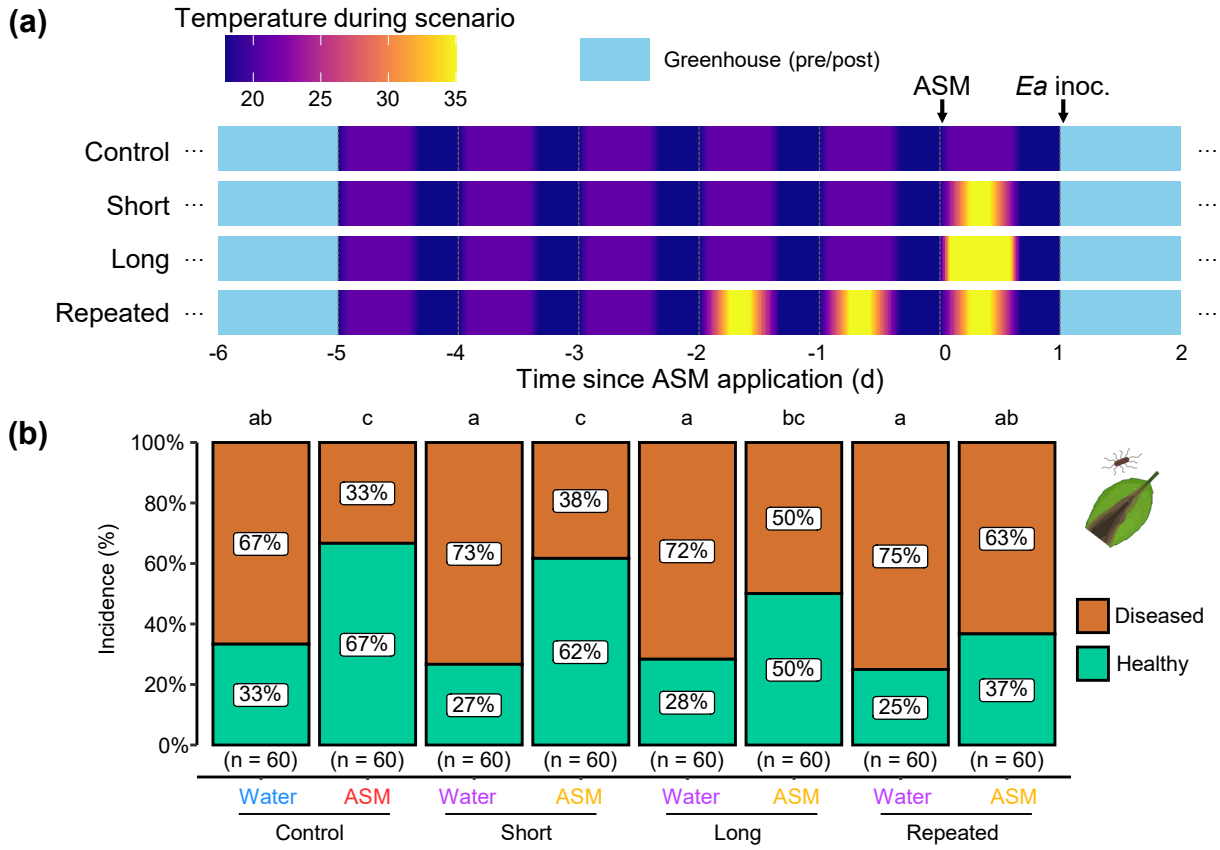


**Fig. 2. Accumulation of high temperatures prior to inoculation impairs the ability of apple seedlings to mount an effective ASM-induced protection against *E. amylovora*. (a)** Schematic representation of the experimental protocol (details in Methods). Air temperature during the contrasting thermal scenario (period in the growth chamber) is color-coded according to the color map. Arrows indicate the application of ASM (or water) treatment and pathogen inoculation on the youngest unfolded leaf. **(b)** Stacked bar chart of seedlings showing the proportion of healthy (asymptomatic) and diseased (symptomatic) seedlings inoculated with *E. amylovora*, 21 d post-inoculation. Data represent 60 biological replicates from 3 independent trials (n = total number of plants). Statistical significance was determined using pairwise Fisher's exact tests; same letters indicate groups that are not significantly different. Icons created in BioRender.com.

Figure 3

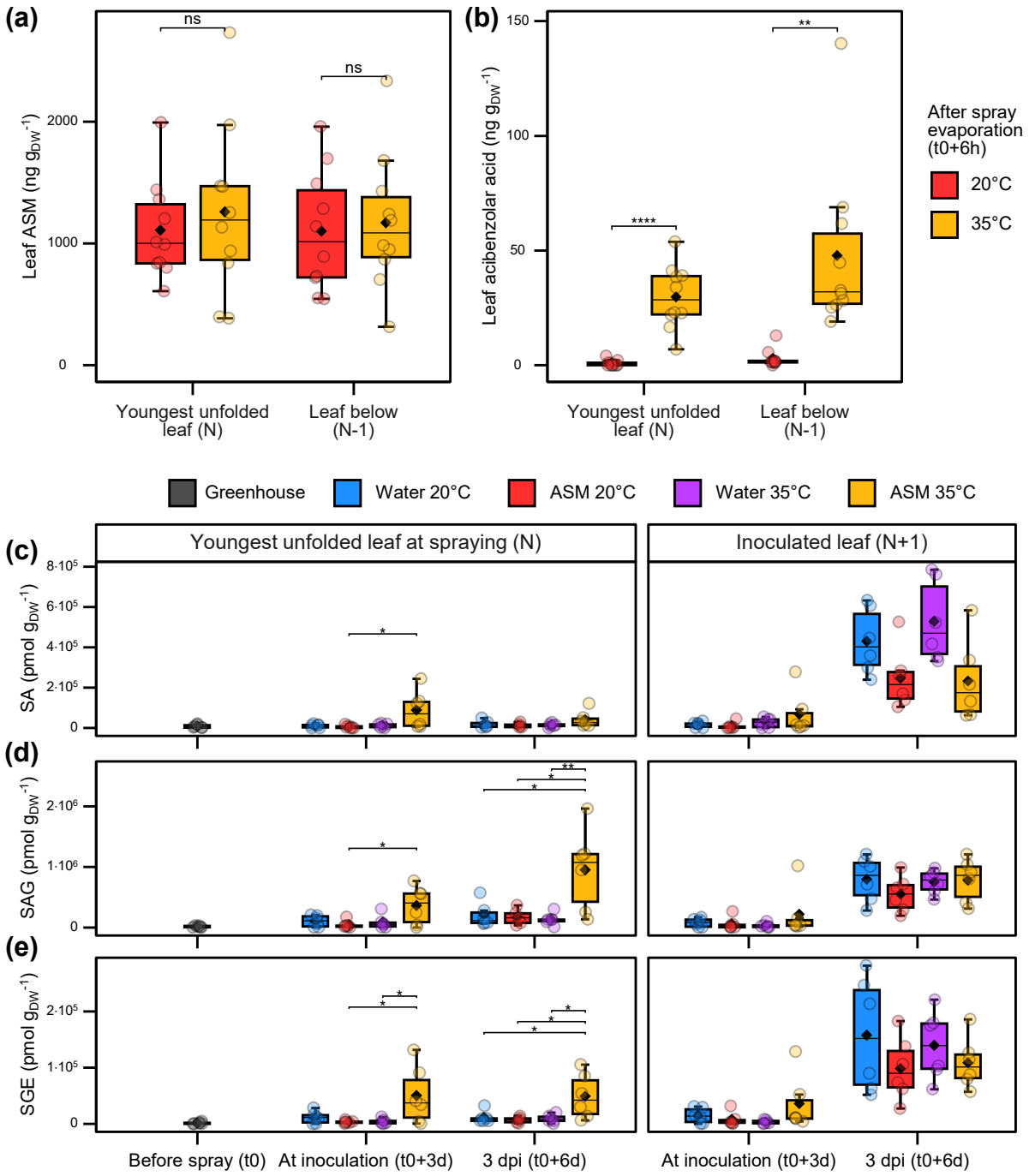


**Fig. 3. High temperature does not alter ASM uptake or SA metabolism in apple seedlings. (a)** and **(b)** Content of ASM and acibenzolar acid (biologically-active catabolite) in the lamina of ASM-treated leaves (n = 10, each pooled from 2 different plants). Apple seedlings were sprayed with ASM ($t_0$) and immediately transferred into a chamber at 20°C or 35°C. The youngest fully unfolded leaf (rank N) and the leaf below (rank N-1) were sampled after 6 h (when the sprayed solution had evaporated) and thoroughly rinsed before quantification of **(a)** ASM and **(b)** acibenzolar acid. **(c)**, **(d)** and **(e)** Content of salicylates in the lamina of water- or ASM-treated leaves (n = 6, each pooled from 8 different plants). Apple seedlings were sprayed with water or ASM ($t_0$) and immediately transferred into a chamber at 20°C or 35°C for 24 h, before being placed in a greenhouse. Three days after spraying ($t_0$+3d), half of the plants was sampled for the youngest fully unfolded leaf at time of spraying (rank N) and the leaf above (rank N+1), while the other half was inoculated with *E. amylovora* at leaf N+1. At three days post-inoculation (3 dpi, $t_0$+6d), the inoculated leaf N+1 and leaf N were harvested. A batch of plants was also harvested for leaf N just before $t_0$, in the greenhouse where the seedlings were grown. The samples were quantified for **(c)** salicylic acid (SA), **(d)** SA glucoside (SAG) and **(e)** SA glucose ester (SGE).

# Figure 4

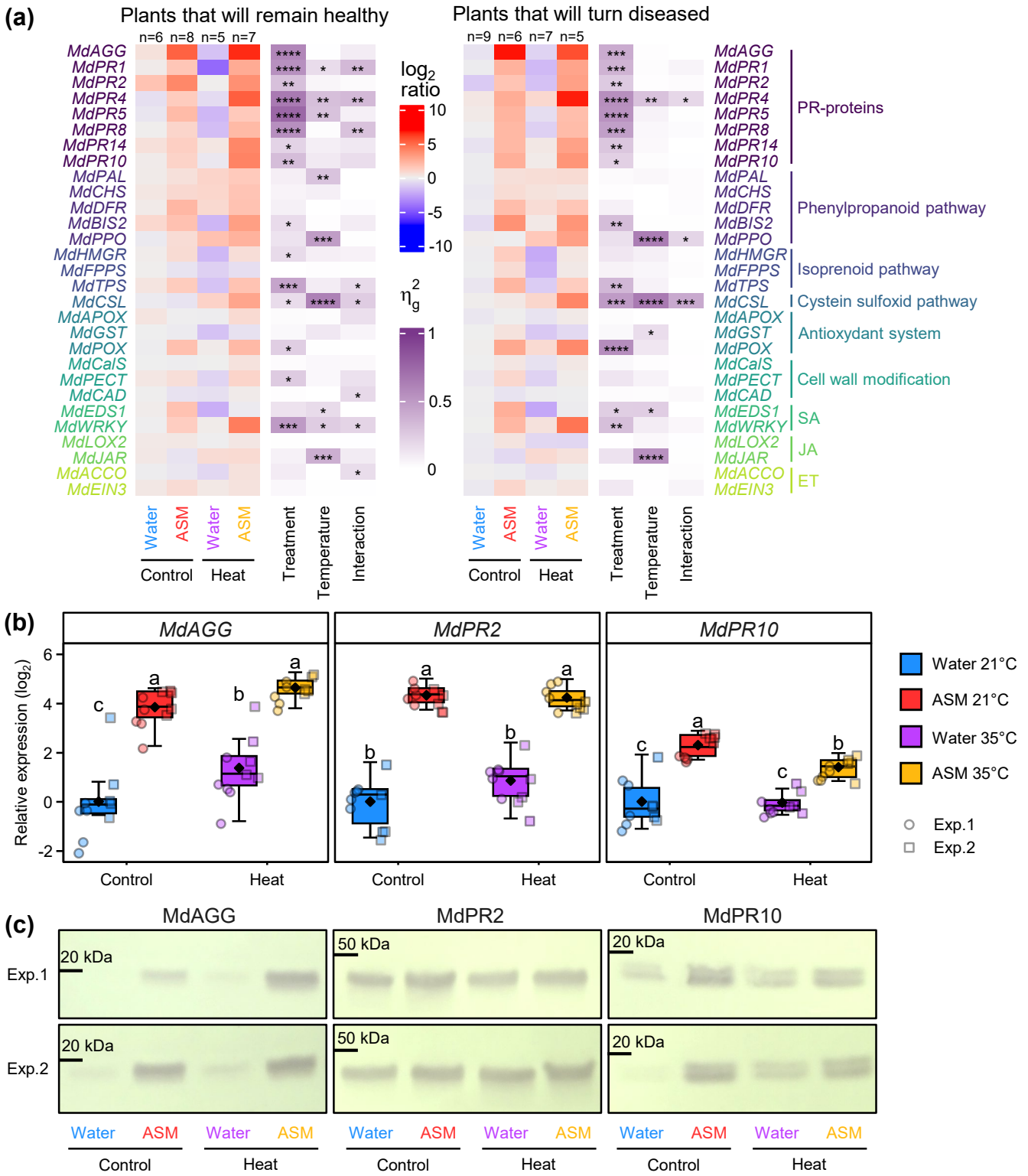


**Fig. 4. High temperature does not prevent ASM-induction of defense markers. (a)** Retrospective transcriptional analysis of 29 marker genes covering a broad range of apple defense mechanisms. Following a scenario similar as in Fig. 1a, young leaves of apple seedlings were individually sampled while inoculating with *E. amylovora*, and grouped *a posteriori* depending on the healthy or diseased fate of their corresponding plant. Heatmaps show relative gene expression and ANOVA effect sizes ($\eta_g^2$) of treatment, temperature and their interaction, as well as their respective significance level (*P<0.05, **P<0.01, ***P<0.001, ****P<0.0001), for both types of plants. Expression values of the average of water-treated leaves from healthy and diseased plants exposed to 20°C were used for the calculation of the $\log_2$ ratio. Expression values were obtained from 5–9 biological replicates (pools of 2 to 4 youngest unfolded leaves at time of ASM or water treatment) from a single trial. **(b)** Relative expression of *MdAGG*, *MdPR2* and *MdPR10* from two independent experiments performed in the same conditions as in Fig. 5a (3-d heatwave, GDDH13 grafted plants – see afterwards). The youngest unfolded leaf at time of sampling was collected from 5 plants per experiment. **(c)** Protein immunodetection of defense-associated proteins. Equal quantities (10 µg) of each protein sample were loaded and run in three separate SDS-PAGE gels. Following transfer to PVDF membranes, each blot was probed with the appropriate primary antibody to detect MdAGG, MdPR2, and MdPR10. Each sample corresponds to a pool of proteins extracted from the 5 biological replicates per experiment presented in **(b)**.

Figure 5

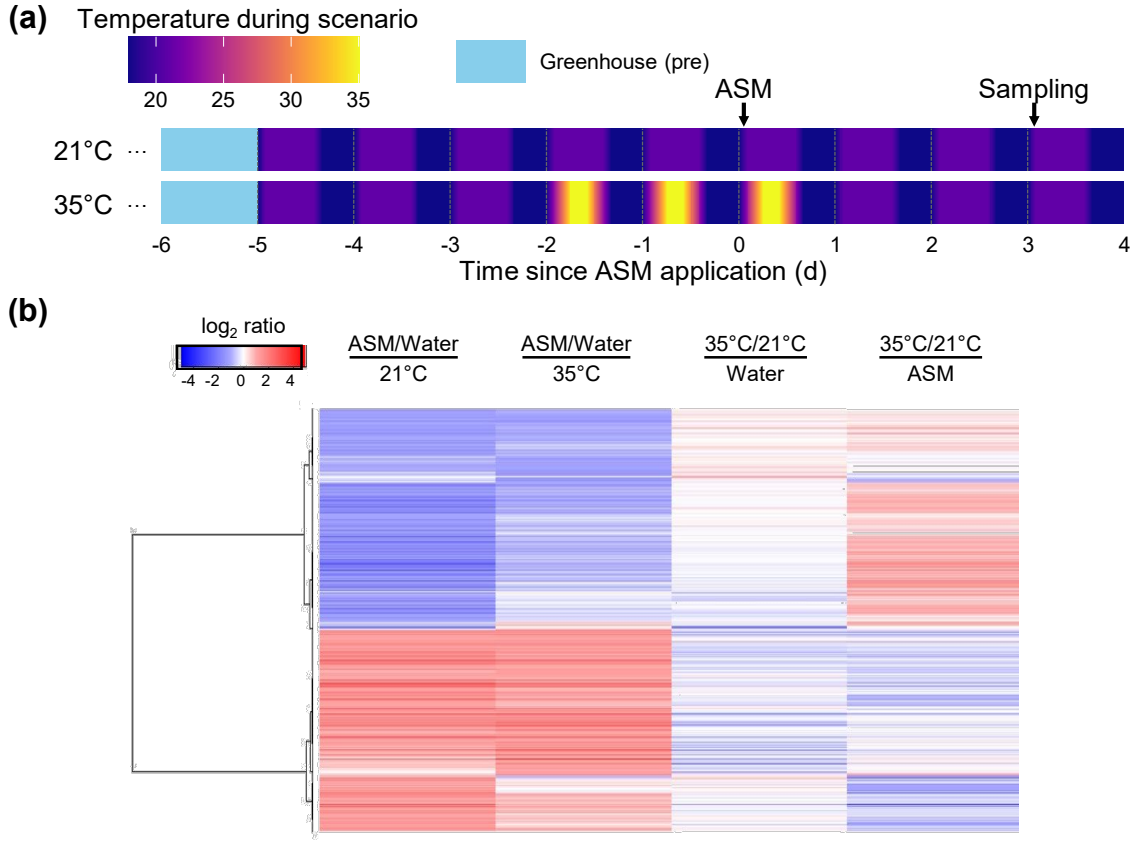


**Fig. 5. High temperature dampens transcriptomic response to ASM. (a)** Schematic diagram of the experimental protocol. Air temperature during the contrasting thermal scenario (period in the growth chamber) is color-coded according to the color map. Arrows indicate the application of ASM or water treatment and the sampling of the youngest unfolded leaf of GDDH13 grafted plants dedicated to microarray analysis. **(b)** Heatmap of 3108 DEGs identified in at least one microarray comparison. DEGs were defined by a $|\log_2 \text{ratio}| \geq 1$ and $P < 0.05$. The hierarchical clustering dendrogram was constructed from the dissimilarity matrix. Expression values were obtained from 2 biological replicates (each pooled from the youngest fully expanded leaf of 4 grafted plants) from 2 independent trials.

Figure 6

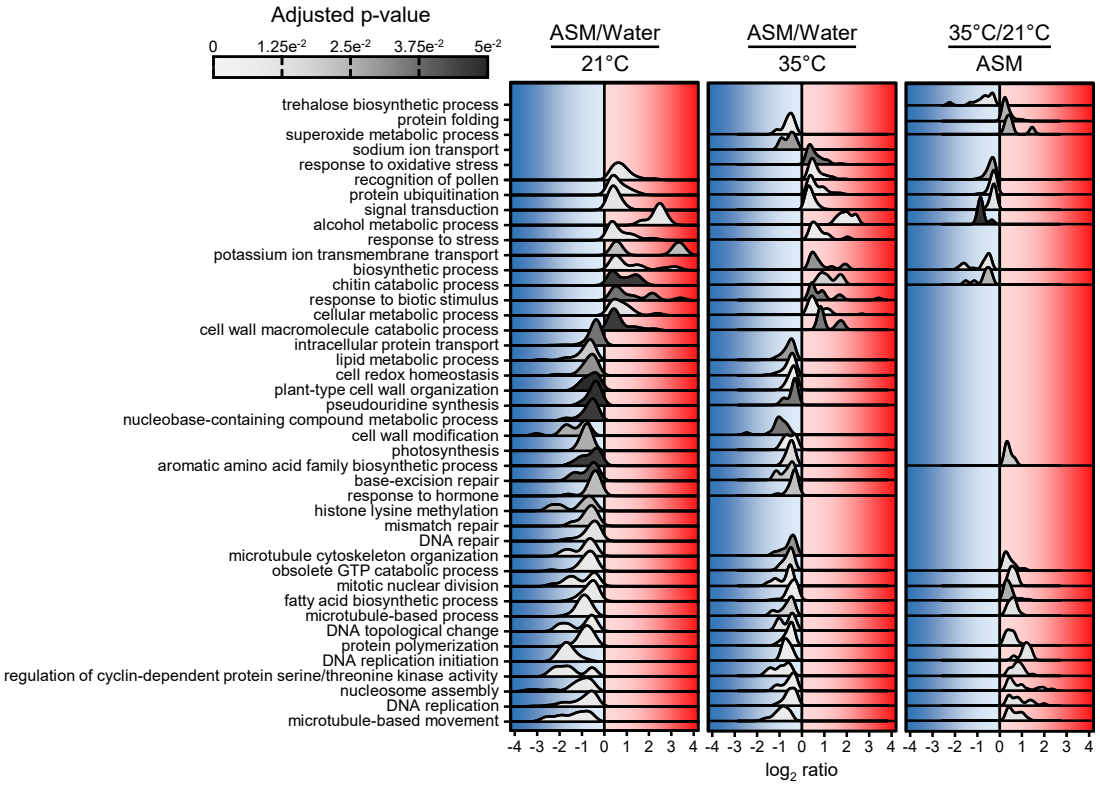


**Fig. 6. Biological processes affected by high temperature during ASM-induced transcriptomic changes are not focused on defense.** Ridgeline plot of GSEA on biological process ontology performed on comparison ASM/water for plants exposed to both 21°C and 35°C and 35°C/21°C comparison for ASM-treated plants. GSEA was obtained by 10.000 permutations with Benjamini and Hochberg procedure for p-value adjustment.

Figure 7

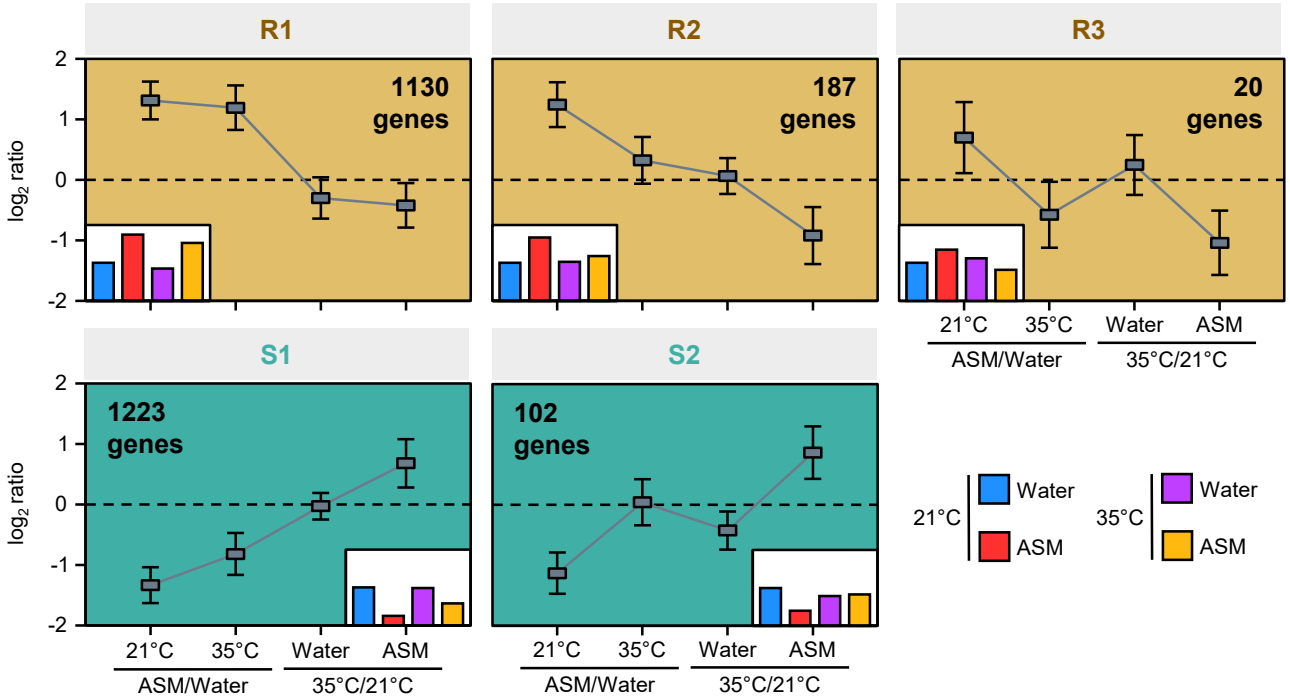


**Fig. 7. Identification of "resistance-associated" and "susceptibility-associated" marker genes by clustering.** CAST clustering performed on the 3108 DEGs (Table S1 and Fig. S5) yielded several clusters evocative of resistant (R1, R2 and R3) and susceptible (S1 and S2) marker genes. The average pattern of expression ratio (± sd) is shown for each cluster. The number of DEGs in each resistance or susceptibility cluster are indicated in the upper right- or left-hand corner, respectively. To facilitate the interpretation of the variations in ratios, barplots showing the inferred expression pattern relative to the control (water, 21°C) are placed in the lower left- or right-hand corner of resistance and susceptibility clusters, respectively.

Figure 8

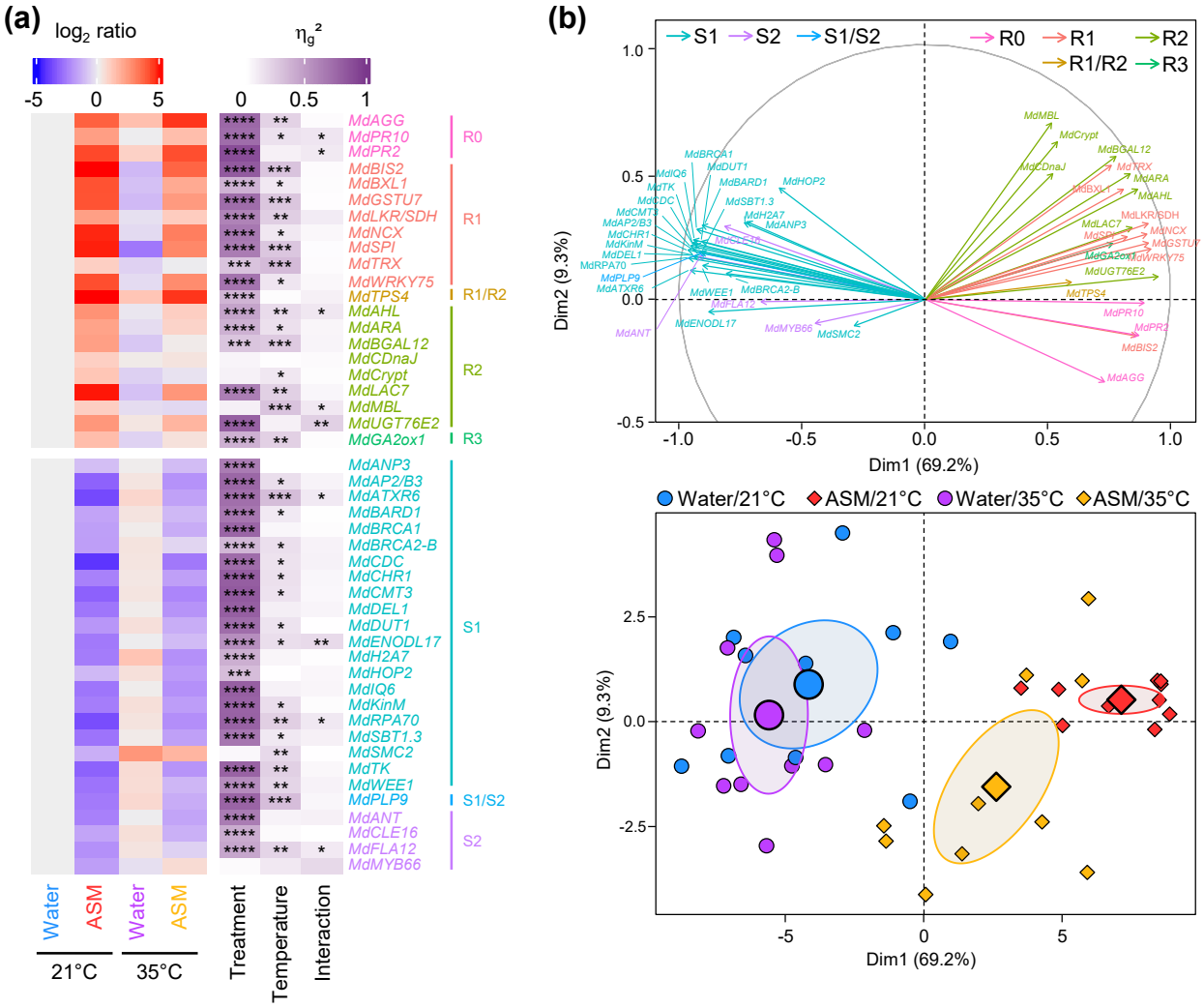


**Fig. 8. High temperature erodes ASM-induced transcriptional regulation of resistance- and susceptibility-associated marker genes.** Expression values of water-treated leaves from plants exposed to 21°C were used for the calculation of the $\log_2$ ratio. Expression values were obtained from 10 biological replicates equally from 2 independent trials. **(a)** Heatmap showing relative gene expression and ANOVA effect sizes ($\eta_g^2$) of treatment, temperature and their interaction, as well as their respective significance level (*P<0.05, **P<0.01, ***P<0.001, ****P<0.0001). **(b)** PCA representation of relative gene expression on the two first dimensions, with the contribution of markers color-coded according to their cluster (top) and the distribution of samples grouped by treatment and temperature (bottom). Ellipses correspond to 95% confidence intervals around the centroid. Note that a single marker may be assigned to several clusters if the corresponding primer targets several homologous genes (Table S2).

Figure 9

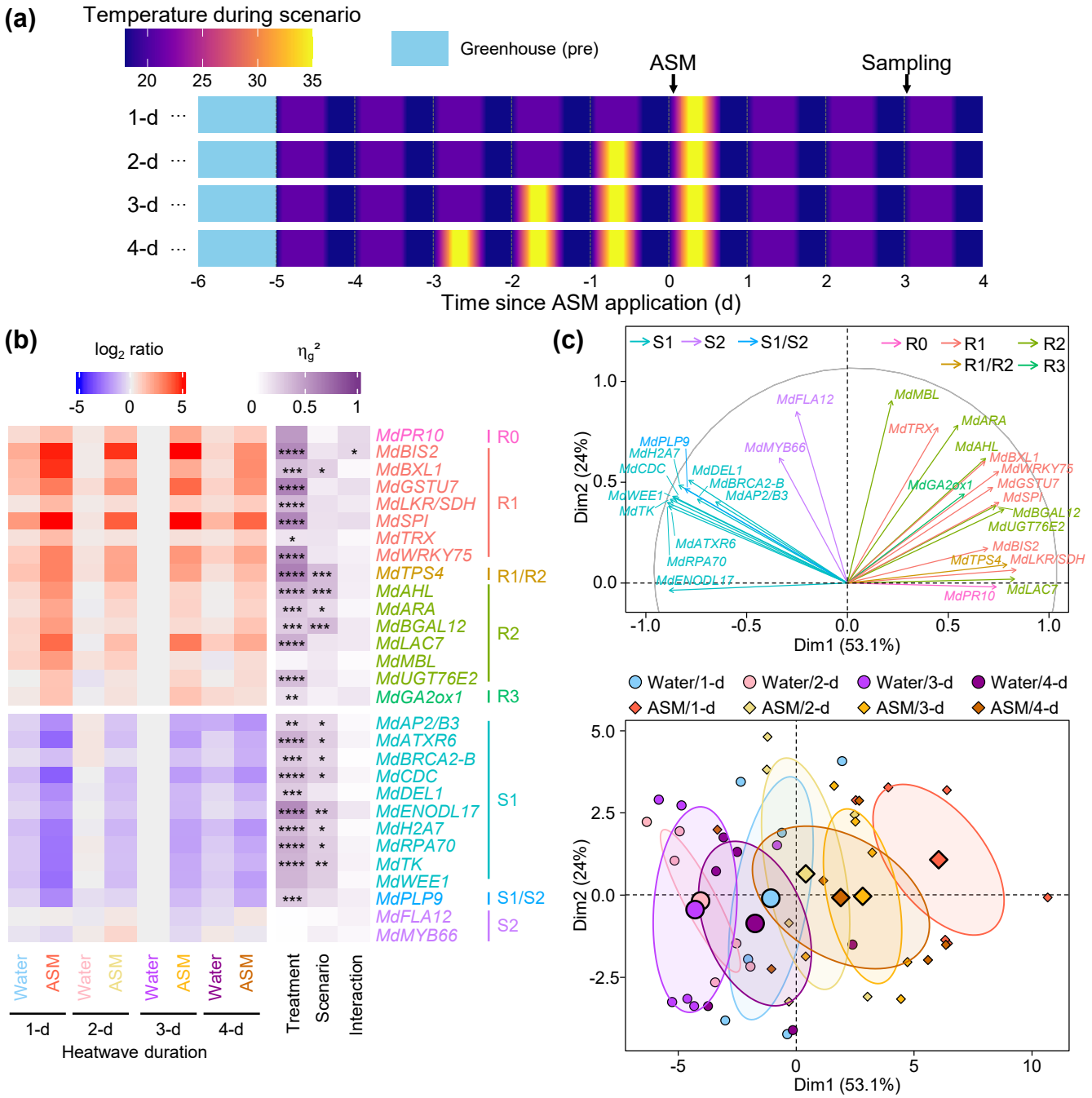


**Fig. 9. The duration of heat exposure before ASM treatment moderately affects the dampening of ASM-induced transcriptional regulation.** Effect of heat duration prior to treatment on the expression of selected markers 3 d after ASM or water treatment, in grafted plants subjected to a 1-d, 2-d, 3-d and 4-d heatwave at 35°C. Expression values of water-treated leaves from plants exposed to 3-d 35°C were used for the calculation of the $\log_2$ ratio. Expression values were obtained from 6 biological replicates equally from 2 independent trials. **(a)** Schematic diagram of the experimental protocol. Air temperature during the contrasting thermal scenario (period in the growth chamber) is color-coded according to the color map. Arrows indicate the application of ASM (or water) treatment and the sampling of the youngest unfolded leaves. **(b)** Heatmap showing relative gene expression and ANOVA effect sizes ($\eta_g^2$) of treatment, temperature and their interaction, as well as their respective significance level (*P<0.05, **P<0.01, ***P<0.001, ****P<0.0001). **(c)** PCA representation of relative gene expression on the two first dimensions, with the contribution of markers color-coded according to their cluster (top) and the distribution of samples grouped by treatment and temperature (bottom). Ellipses correspond to 95% confidence intervals around the centroid. Note that a single marker may be assigned to several clusters if the corresponding primer targets several homologous genes (Table S2).

Figure 10

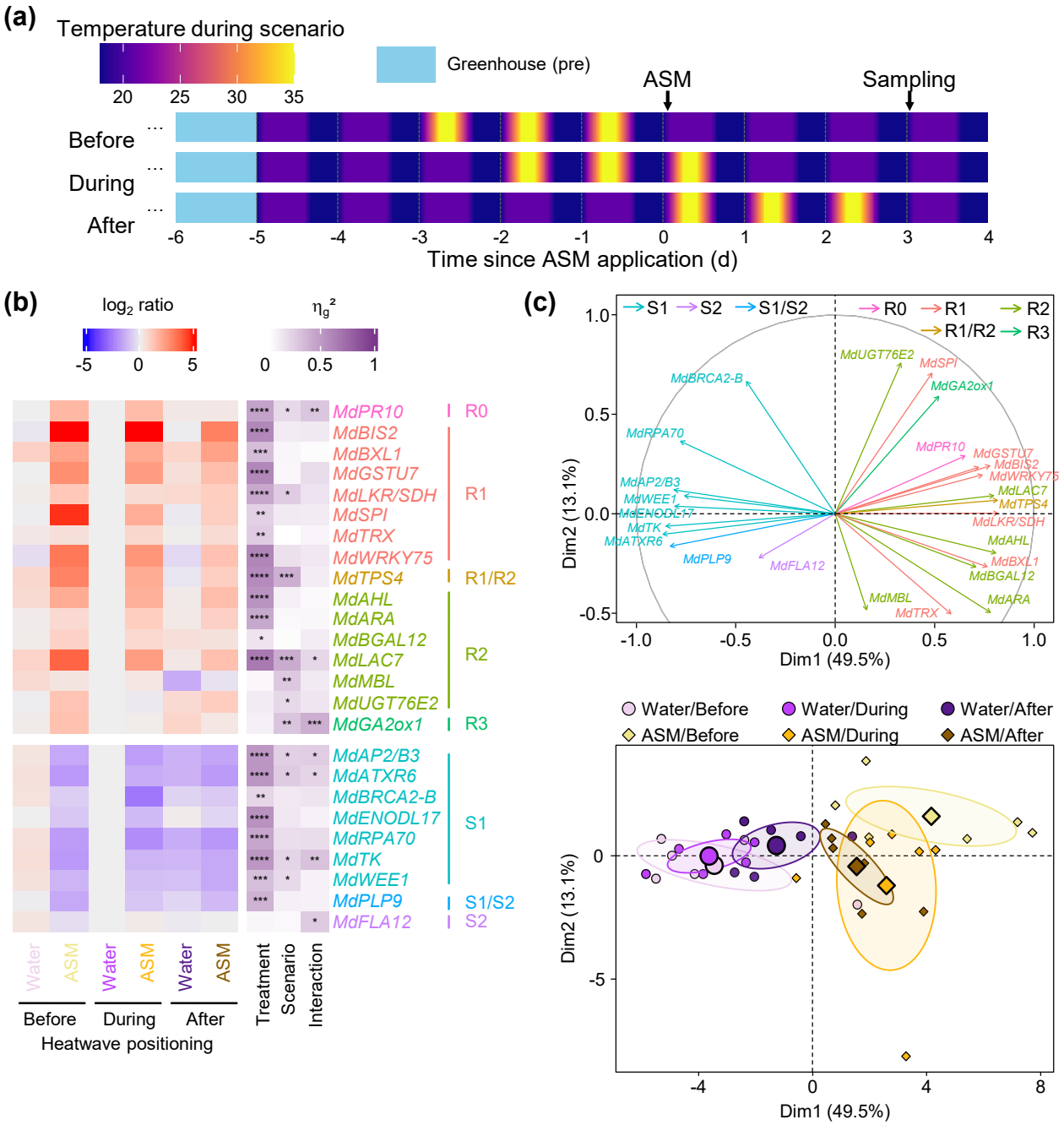


**Fig. 10. A heatwave posterior to ASM application dampens ASM-induced transcriptional regulation more strongly than a prior heatwave.** Effect of heatwave positioning on expression of selected markers 3 d after ASM or water treatment, in grafted plants subjected to a 3-d heatwave at 35°C before, during or after ASM or water treatment. Expression values of water-treated leaves from plants under heatwave during the treatment were used for the calculation of the $\log_2$ ratio. Expression values were obtained from 6 biological replicates equally from 2 independent trials. **(a)** Schematic diagram of the experimental protocol. Air temperature during the contrasting thermal scenario (period in the growth chamber) is color-coded according to the color map. Arrows indicate the application of ASM (or water) treatment and the sampling of the youngest unfolded leaves. **(b)** Heatmap showing relative gene expression and ANOVA effect sizes ($\eta_g^2$) of treatment, temperature and their interaction, as well as their respective significance level (*P<0.05, **P<0.01, ***P<0.001, ****P<0.0001). **(c)** PCA representation of relative gene expression on the two first dimensions, with the contribution of markers color-coded according to their cluster (top) and distribution of samples grouped by treatment and temperature (bottom). Ellipses correspond to 95% confidence intervals around the centroid. Note that a single marker may be assigned to several clusters if the corresponding primer targets several homologous genes (Table S2).

Figure 11

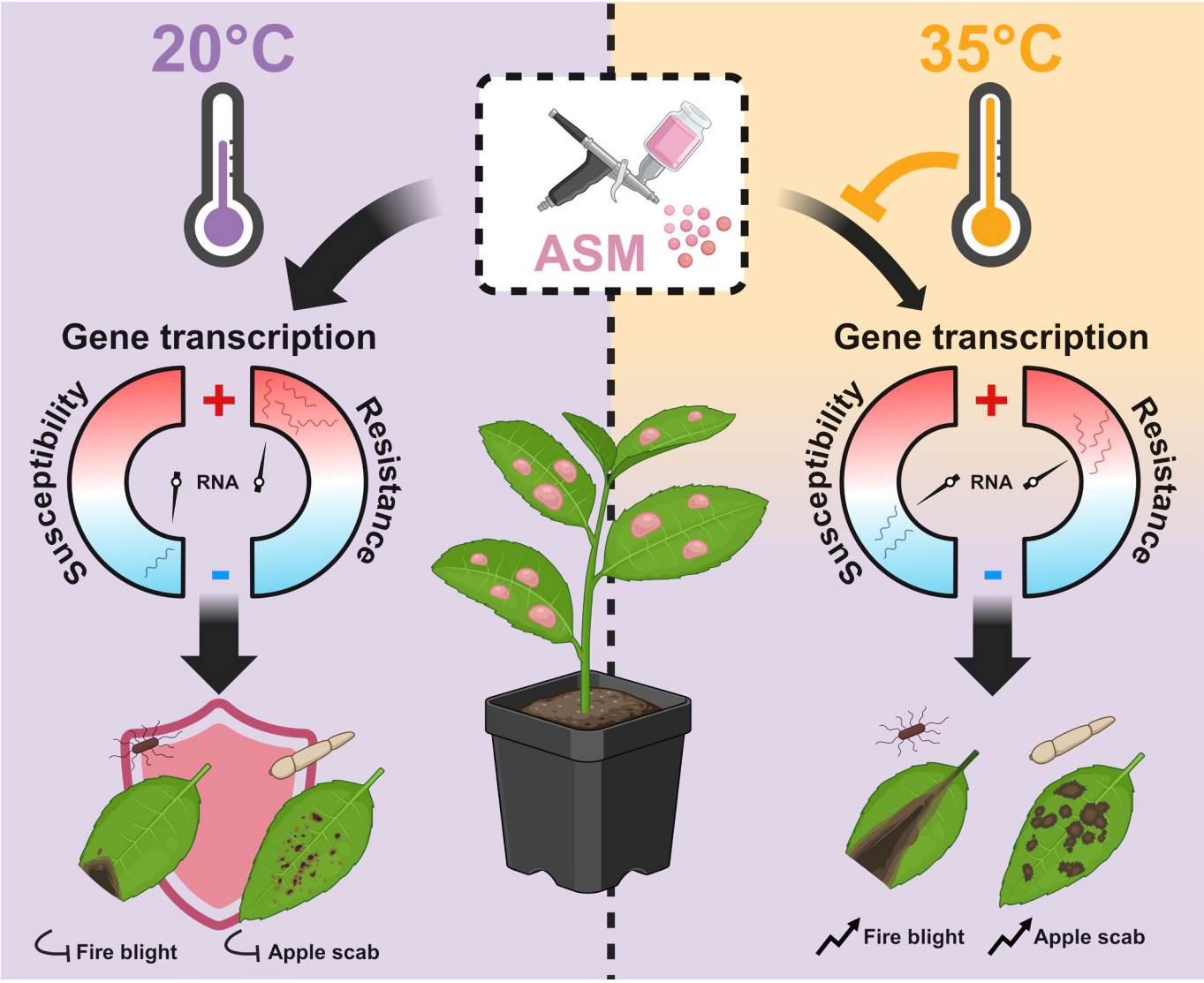


**Fig. 11. Working model for the loss of ASM-induced protection of apple plants upon transient heat.** At control temperature (20°C), spraying apple plants with ASM prior to inoculation with the bacteria *E. amylovora* or the fungus *V. inaequalis* allows apple leaves to mount an effective transcriptional response whereby resistance-associated genes are up-regulated and susceptibility-associated genes are down-regulated – which reduces the incidence of fire blight or apple scab. When a heatwave (35°C) occurs in between ASM application and pathogen inoculation, ASM-induced transcriptional regulation is dampened, ultimately enabling pathogens to proliferate. Created in BioRender.com.